GDCh Research Article Angewandte International Edition Chemie www.angewandte.org

How to cite: *Angew. Chem. Int. Ed.* **2025**, e202500649
doi.org/10.1002/anie.202500649

DNA Nanotechnology

Conformationally Locked Peptide–DNA Nanostructures for CRISPR-Amplified Activity-Based Sensing

*Dylan M. Snider, Mackenzie L. Coffin, Brian J. Armijo, Ryan Khetan, Mark W. Duchow, Anna Capasso, and Devleena Samanta**

Abstract: We introduce a new class of chemical probes for activity-based sensing of proteases, termed cleavable, locked initiator probes (CLIPs). CLIPs contain a protease-cleavable peptide linked between two programmable DNA strands—an "initiator" DNA and a shorter "blocking" DNA. These DNA sequences are designed to hybridize, creating a "locked" hairpin-like structure. Upon proteolytic cleavage, the initiator strand is released, triggering the activation of CRISPR-Cas12a enzymes and producing an amplified fluorescence response. CLIPs generate more than 20-fold turn-on signals at room temperature (25 °C), significantly outperforming commercial probes by yielding ~40-fold lower limits of detection (LOD) at 100-fold lower concentrations. Their versatility enables the detection of various disease-relevant proteases—including the SARS-CoV-2 main protease, caspase-3, matrix metalloproteinase-7, and cathepsin B—simply by altering the peptide sequence. Importantly, CLIPs detect cathepsin B in four different colorectal cancer cell lines, highlighting their clinical potential. Taken together, the sensitivity (LOD: ~88 pM), selectivity, and rapid assay time (down to 35 min), combined with the ability to operate in complex biological media with minimal sample preparation, position CLIPs as powerful chemical tools for activity-based sensing of functional enzymes.

Introduction

Fluorescent probes, such as molecular beacons (MBs), have revolutionized biomolecule detection, enabling significant advancements in diagnostic technologies.[1–3] MBs typically function through a hairpin-shaped DNA structure that, when hybridized with a complementary target nucleic acid, separates a fluorophore-quencher pair, leading to a detectable increase in fluorescence signal. This mechanism has made molecular beacons an essential tool in nucleic acid detection, finding applications in cancer diagnostics, infectious disease monitoring, and personalized medicine.[4–7]

Seitz, Grossmann, and others have extended the utility of this technology to protein detection through the development of peptide beacons.[8–13] These modified probes comprise a peptide in the loop region of the hairpin that changes conformation in response to protein binding, enabling the detection of protein biomarkers rather than nucleic acids. This innovation significantly broadens the scope of molecular beacons, allowing for their application in protein-based diagnostics, thereby opening new avenues in early disease detection.[8]

A key limitation of these beacon-type structures is the lack of a handle for signal amplification. In most cases, the interaction between the probe and the target is binding-based and occurs in 1:1 ratio that makes detecting low concentrations of targets challenging, thereby limiting the sensitivity of the assay. Additionally, binding-based probes are unable to distinguish between the active and inactive forms of biomolecules, which is a critical drawback in applications where only the active form is biologically relevant.

Activity-based sensing offers a powerful alternative to traditional binding-based methods, significantly enhancing diagnostic potential.[14–16] In this report, we present the development of a new class of chemical probes—cleavable, locked initiator probes (CLIPs). These probes consist of a DNA–peptide–DNA triblock, conformationally locked into a hairpin nanostructure that resembles MBs but enables activity-based sensing and incorporates a handle for CRISPR-amplified signal generation. CRISPR-based sensing is chosen due to its ease of use and ability to detect targets at sub-picomolar levels under isothermal conditions.[17–21]

We show the functionality of CLIPs for detecting active proteases. We focus on proteases because of three primary reasons. First, they are often expressed in inactive precursor forms and are only activated under specific physiological conditions. Therefore, probes that can selectively detect the active form are required. Second, dysregulation of protease activity has been shown to be linked to various conditions, such

[*] D. M. Snider, M. L. Coffin, B. J. Armijo, R. Khetan, D. Samanta
Department of Chemistry, The University of Texas at Austin, 105 E 24th St., Austin TX 78712, USA
E-mail: dsamanta@utexas.edu

M. W. Duchow, A. Capasso
Department of Oncology, Dell Medical School, The University of Texas at Austin, 1601 Trinity St., Austin TX 78712, USA

D. Samanta
Livestrong Cancer Institutes, Dell Medical School, The University of Texas at Austin, 1601 Trinity St., Austin TX 78712, USA

D. Samanta
Texas Materials Institute, The University of Texas at Austin, 2501 Speedway, Austin TX 78712, USA

Additional supporting information can be found online in the Supporting Information section

as cancers,[15,22,23] infectious diseases,[24] neurodegenerative disorders,[25,26] inflammatory conditions,[27] and cardiovascular diseases.[28] Activity-based protease sensing has shown great promise in improving diagnostic and prognostic tools for these conditions.[15,16,22–24,29–35] Third, detecting active proteases presents significant challenges. Traditional methods use peptide substrates that are labeled with reporters and can be cleaved by proteases of interest after which, the fragments are monitored through spectroscopy or mass spectrometry.[36,37] Although these methods can indicate protease activity, they come with several limitations. They often require elevated temperatures, suffer from limited sensitivity, involve extensive sample processing, and depend on advanced instrumentation. Additionally, they typically necessitate high concentrations of both the substrate and the protease to generate a detectable signal, which diminishes their effectiveness in detecting low-abundance or weakly active proteases. This issue becomes especially critical in biological contexts, where local protease concentrations can be relatively high (up to ~mM),[38] but their levels in biofluids such as serum are much lower (~pM–nM),[39,40] making detection even more challenging. Consequently, more sensitive methods are needed to address these complexities in protease detection in clinical and diagnostic settings.

We and others have previously shown that CRISPR-based approaches can enhance the detection of active proteases.[41–43] However, there are still key challenges that remain. Some methods require complex and costly synthetic biology, which necessitates specialized expertise.[43–45] Several approaches need elevated temperatures (above room temperature) for operation.[43–45] Recently-developed nanoparticle-based approaches necessitate a separation step to differentiate between intact and cleaved peptides, adding complexity and increasing the risk of losing cleaved substrates.[41,42,46] Furthermore, peptides presented on nanoparticle surfaces can be sterically hindered, limiting their accessibility to proteases. To overcome this, longer peptides (>10 amino acids) or spacers are often required to ensure efficient cleavage, complicating sensor design and reducing performance.[41,47] The CLIP structure introduced herein overcomes these limitations, enabling one-pot detection of proteases at room temperature with commonly available instrumentation such as plate readers.

Results and Discussion

Design and Structural Characterization of CLIPs

The CLIP structure comprises three key components (Figure 1a–c): 1) a peptide domain that is specifically recognized and cleaved by the target protease, 2) an "initiator" DNA sequence that is capable of activating a CRISPR-Cas12a ribonucleoprotein (RNP) complex,[17,20] and 3) a short "blocking" DNA strand. This blocking strand hybridizes with the initiator sequence to form a locked, hairpin-like nanostructure with a melting temperature (T_m) significantly above room temperature, ensuring that the probe remains inactive until specific protease-mediated cleavage occurs.

We hypothesized that this locked state would sterically hinder the CRISPR-Cas12a RNP complex from interacting with the initiator strand, thereby preventing signal transduction in the absence of active proteases (Figures S1 and S2). Upon cleavage of the peptide by the target protease, the probe undergoes a conformational shift from an intramolecular DNA duplex (locked state) to an intermolecular DNA duplex (unlocked state). This structural change lowers the T_m of the duplex, causing the blocking strand to spontaneously dissociate from the initiator strand (Figure 1d). The freed initiator DNA then activates the CRISPR-Cas12a RNP complex, which, in combination with fluorophore-quencher labeled DNaseAlert reporters, generates an amplified fluorescence signal (Figure 1e), significantly enhancing the detection of active proteases.[17,20]

As a proof-of-concept, we created a CLIP for detecting the 3-chymotrypsin-like main protease (3CL) of SARS-CoV-2. 3CL was chosen as the model protease because it is relevant for detecting active SARS-CoV-2 infections and has a well-defined substrate.[48–50] The peptide sequence (Table S1), CSAVLQ↓SGFK(N_3), was modeled after a commercially available 3CL substrate[51] and was modified with a C-terminal azido-lysine. This modified peptide was chemically linked to a 24-nt initiator sequence (Table S2) equipped with dibenzocyclooctyne (DBCO) at the 5′ end, utilizing click chemistry. The final DNA–peptide–DNA triblock structure was synthesized by adapting a recently developed proximity-based approach (Figure S3).[52] We note that alternative synthetic strategies, such as bead-based approaches could also be used to synthesize such triblock structures.[53]

The desirable length of the blocking DNA was determined computationally using the IDT OligoAnalyzer tool (Figure S4; Tables S3–S6). Specifically, we modeled hairpins composed entirely of DNA, with contour lengths similar to those of the CLIPs, and then calculated their T_m. Additionally, we computed the T_m of just the stem portions to simulate the structure after proteolytic digestion of the CLIPs. Our computational screening of 264 different conditions, including varying DNA concentrations, ionic strengths, and different stem and loop sizes, indicated that an 8-nt blocking DNA is ideal. This length would allow the CLIP to form a stable hairpin structure at 25 °C and to spontaneously separate into single-stranded DNA after proteolytic cleavage, facilitating detection.

The synthesized CLIPs were characterized using MALDI-MS (Tables S7 and S8), UV–vis spectroscopy (Figures S5 and S6), and gel electrophoresis (Figure S7). To confirm that proteases can cleave CLIPs, we incubated 3CL-CLIP with excess 3CL protease overnight and analyzed the sample using MALDI-MS (Figure 2a). The intact 3CL-CLIP displayed a dominant peak near its expected mass (calculated *m/z*: 12,569). After treatment with the protease, the probe showed two new peaks, which correspond to the lower-mass fragments produced by the cleavage of the CLIP (calculated *m/z*: 4,273 and 8,313). The cleavage was further supported by gel electrophoresis data (Figure S7).

The hairpin-like structure of the CLIP was confirmed by experimentally determining its T_m (Figure 2b). The T_m of 1 μM of the CLIP was found to be ~53 °C, similar to that

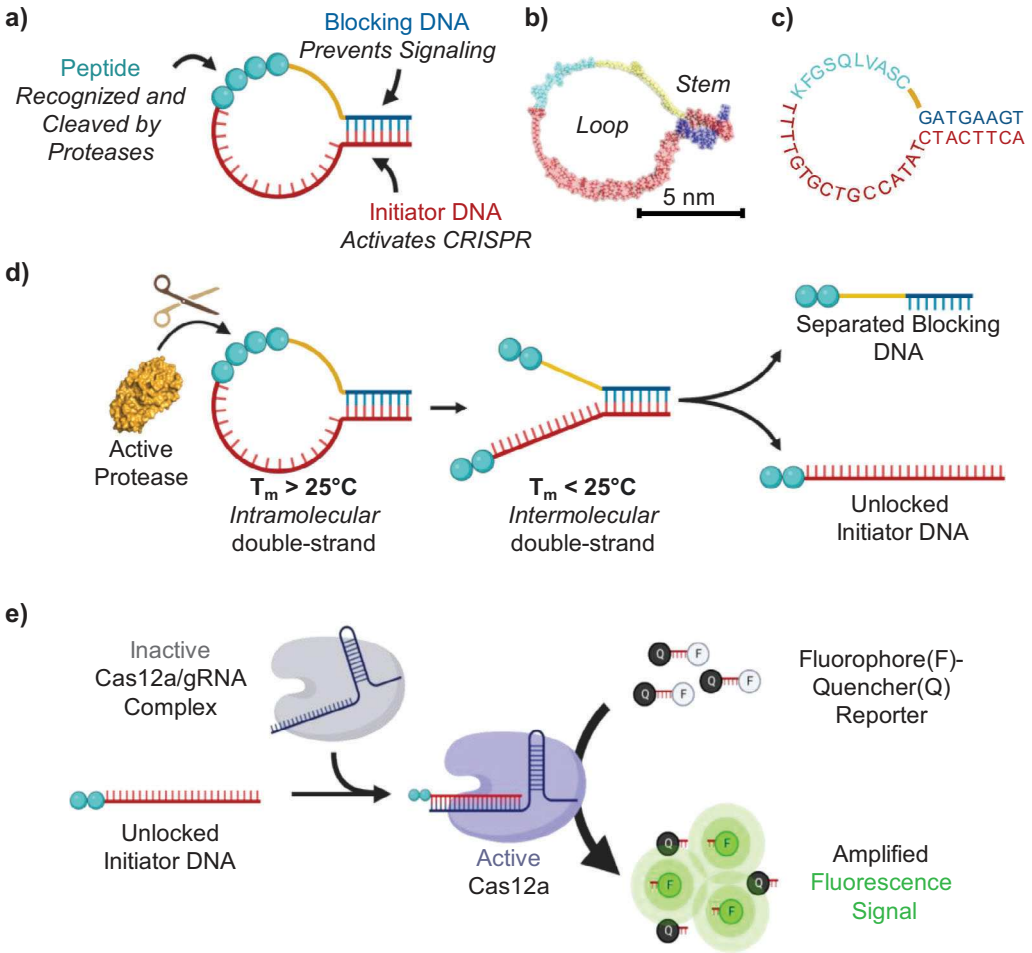

Figure 1. a) Cartoon structure of a CLIP comprising an initiator DNA, peptide, and blocking DNA. b) Molecular model of 3CL-CLIP with an idealized circular loop. c) 3CL-CLIP showing peptide and DNA sequences. d) Schematic showing the mechanism of activation of CLIPs. CLIPs form a locked hairpin-like nanostructure in solution, consisting of an intramolecular DNA double strand. Treatment with a target protease results in the proteolytic cleavage of the peptide substrate. This cleavage transforms the stable hairpin structure into an unstable intermolecular double strand, which has a lower melting temperature. Consequently, the DNA melts, unlocking the initiator DNA for subsequent signal transduction and amplification. e) Scheme for detection of the initiator strand using a CRISPR-Cas12a based assay. Cas12a is complexed with a gRNA with complementarity to the initiator strand to form an inactive RNP. Upon binding, the initiator strand activates the Cas enzyme that then shows indiscriminate endonuclease activity toward single-stranded DNA. This enzymatic activity is monitored using commercial DNaseAlert™ reporters, which consist of single-stranded DNA labeled with a fluorophore and quencher at either end.

of a DNA hairpin of comparable size (Tables S3–S6). This similarity suggests that the CLIP retains its intended locked structure in solution at room temperature. After treatment with protease, however, the T_m of the CLIP dropped to around ~25 °C, which matches the T_m observed for a simple 1:1 mixture of the initiator and blocking strands at the same concentration. This lower T_m indicates that the probe's stability decreases following protease-mediated cleavage.

CLIPs are Activated by Target Proteases

We next investigated the functionality of CLIPs in reporting active proteases at room temperature (Figures S7–S13). After incubating the CLIPs with 500 nM 3CL protease for 30 min, we performed a CRISPR assay and detected a rapid increase in fluorescence within 5 min, yielding results within as quick as 35 min of total assay time. The fluorescence generated was time-dependent and reached a plateau by 3 h (Figure 2c). In contrast, the fluorescence of the probes alone remained largely unchanged. Importantly, the DNA–peptide–DNA triblock structure is essential for seeing this locked behavior. For comparison, DNA-only hairpins with similar loop sizes and stem lengths activate CRISPR (Figures S14–16), suggesting that the initiator sequences in these hairpins remain accessible to the RNP, potentially through strand displacement (Figures S17–S19). This finding underscores the structural uniqueness of CLIPs as conditional CRISPR activators, highlighting their potential utility in a variety of applications.

Next, we benchmarked 3CL-CLIP against a commercial fluorogenic probe (3CL-CFP). 3CL-CFP is a rhodamine-labeled peptide in which the fluorescence of the rhodamine dye is quenched upon conjugation to the peptide. Cleavage

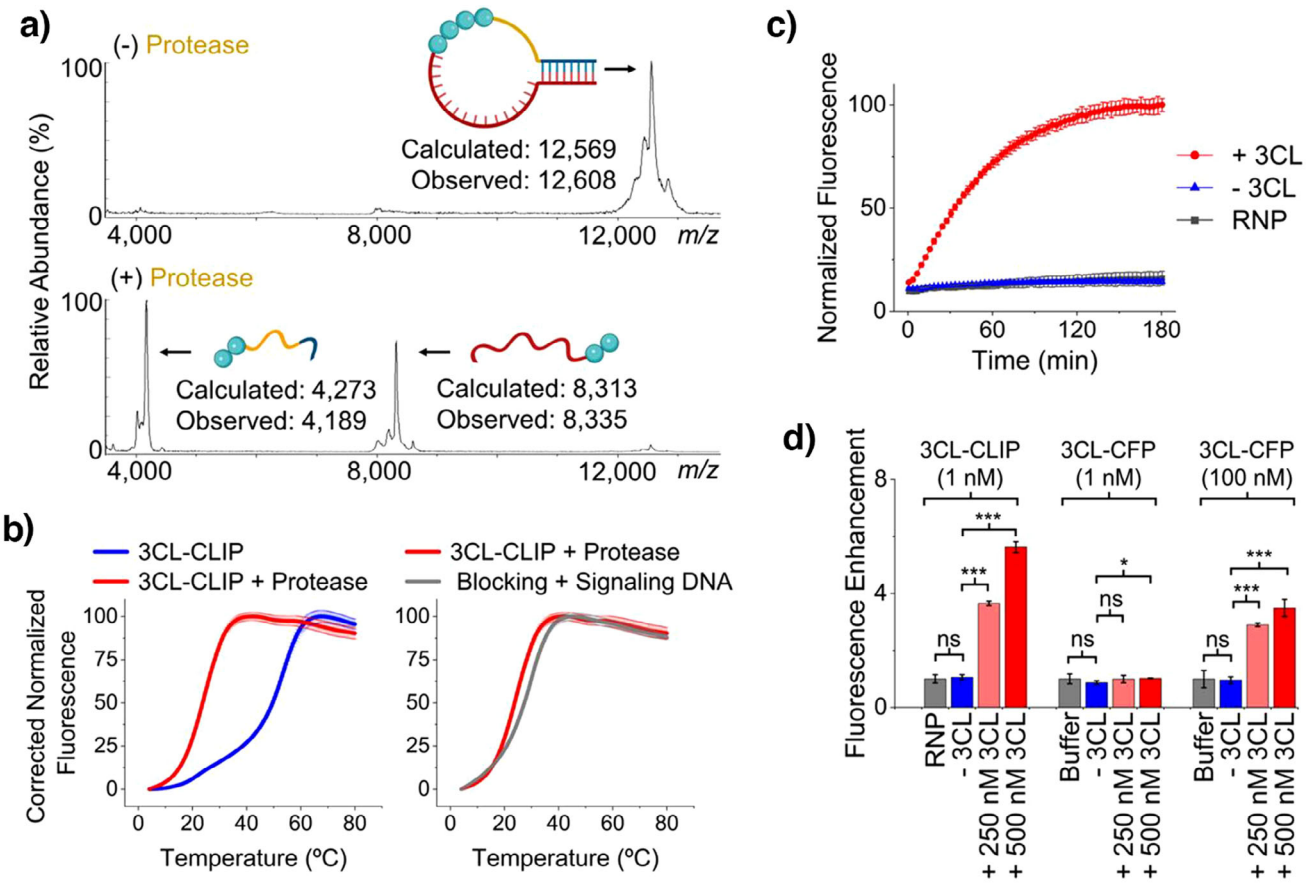

Figure 2. a) MALDI-MS spectra of 3CL-CLIP before and after exposure to 3CL protease. After protease treatment, the peak at 12,569 *m/z* diminishes, and two new fragments, correlating with the expected proteolytic fragments of CLIPs, appear. Relative abundance is calculated by setting the highest *m/z* value to 100%. b) Melting curves of 3CL-CLIP before (blue) and after (red) treatment with 3CL protease, alongside control (gray) consisting of 1:1 mixture of initiator and blocking strands, all at 1 μM concentration. T_m of 3CL-CLIP, initially around ~53 °C, decreases to ~25 °C post-treatment, matching the T_m of the mixture of strands, suggesting a significant alteration in structure and stability due to protease-mediated cleavage. Corrected normalized fluorescence was calculated by setting the maximum and minimum fluorescence values across the data set to 100 and 0, respectively, with adjustments made for the inherent temperature-dependence of the dye's fluorescence. c) CRISPR-mediated detection of 3CL using 3CL-CLIP. Fluorescence signal increases dramatically after 3CL-CLIP is treated 500 nM 3CL protease for 30 min. Normalized fluorescence is calculated by normalizing the highest fluorescence value in a data set to 100%. d) Comparison of 3CL-CLIPs with a commercial fluorogenic 3CL probe (3CL-CFP). Fluorescence enhancement is defined as ratio of the fluorescence values of a sample to the fluorescence of the RNP complex or buffer. * and *** denote statistical significance at the 95% and 99.9% confidence levels, respectively, whereas "ns" indicates no statistical significance (at the 95% confidence level), assessed using a one-tailed Student's *t*-test.

by 3CL protease restores fluorescence, resulting in a turn-on signal. Compared to 3CL-CFP, 3CL-CLIP generated over 1.5-fold greater signal at 100 times lower concentration (Figure 2d). This significant enhancement is attributed to the integration of DNA into the probe's design (Figures S20–S24). We confirmed this by constructing a 3CL-CLIP with a beacon-like structure, where the probe is labeled with a fluorophore at one end and a quencher at the other. Protease-mediated peptide cleavage separates these two elements, triggering a fluorescence signal (Figures S22 and S23). Our findings demonstrate that CRISPR-based signal amplification allows for protease detection at probe concentrations 100 times lower than those required for direct detection using a traditional beacon-like structure (Figure S24).

To assess the versatility of CLIPs, additional probes were synthesized for the proteases cathepsin B (CTSB), matrix-metalloprotease 7 (MMP7), and caspase-3 (CASP3) (Figure 3a). These proteases were chosen due to their significance to cancer biology. Specifically, CTSB and MMP7 are known for their involvement in tumor growth and metastasis[54–58] and CASP3 is essential in the process of apoptosis.[59] Detecting these proteases is vital for enhancing our understanding of cancer mechanisms and for the development of diagnostic platforms. When incubated with their respective proteases, a pronounced increase in fluorescence signal was observed, indicating the successful detection of the target proteases. (Figure 3b).

CLIPs are Sensitive and Selective Protease Sensors

We next evaluated the potential of CLIPs for detecting diagnostically relevant proteases, particularly focusing on CTSB due to its overexpression in various cancers.[54,57,58,60]

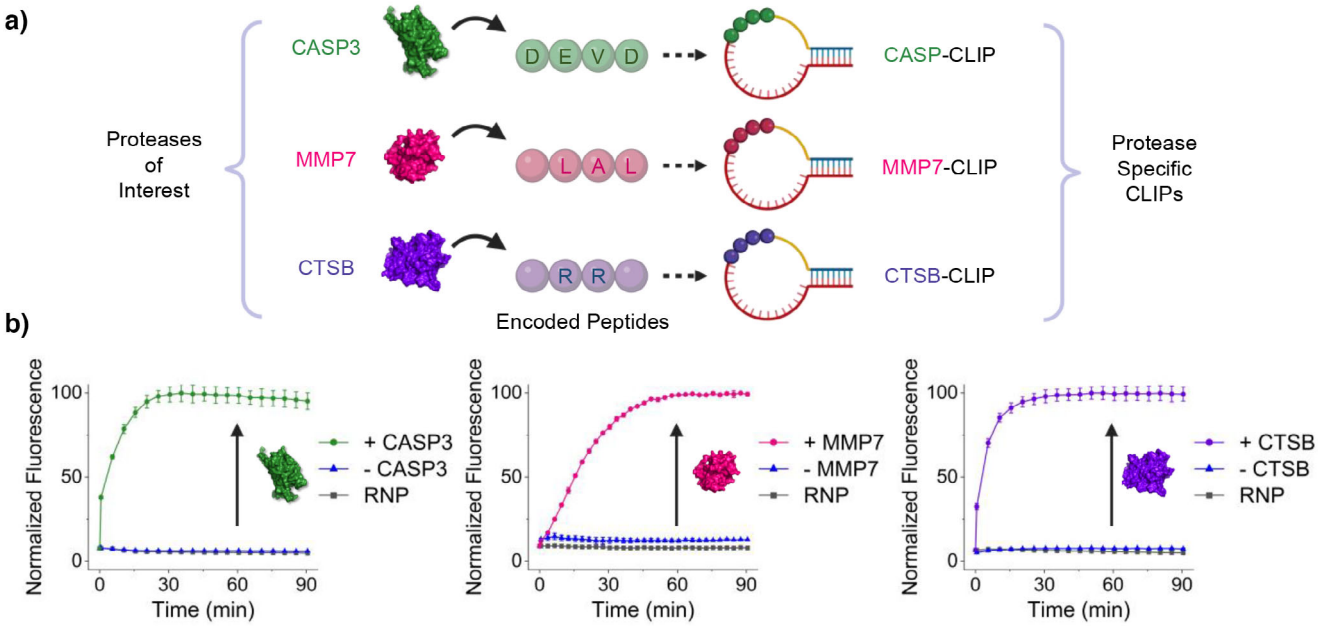

Figure 3. a) Scheme showing design of CLIPs for detecting cancer-relevant proteases, CASP3 (PDB ID:6CKZ), MMP7 (PDB ID:7WXX), and CTSB (PDB ID:1PBH). Amino acid sequences recognized and cleaved by the proteases are highlighted. b) CRISPR-based detection of CASP3, MMP7, and CTSB using CASP3-CLIP, MMP7-CLIP, and CTSB-CLIP, respectively. Due to differences in the intrinsic activities of the proteases, protease concentrations used were 500 nM for CASP3, 250 nM for MMP7, and 20 nM for CTSB, to achieve comparable fluorescence. Normalized fluorescence is calculated by normalizing the highest fluorescence value in a data set to 100%.

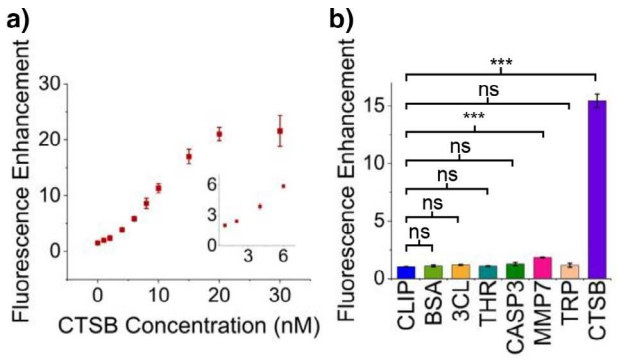

Figure 4. a) Calibration curve showing fluorescence enhancement (defined as fluorescence of CTSB-CLIP treated with CTSB relative to that of RNP alone) observed at the 120 min timepoint in the CRISPR assay versus the concentration of CTSB. LOD was calculated using the $3\sigma/m$ method to be ~88 pM at this time point. b) Specificity assay for CTSB-CLIP when incubated with 20 nM nonspecific proteases and proteins. Substantial fluorescence enhancement is observed preferentially in the presence of CTSB protease. *** denotes statistical significance at the 99.9% confidence levels, whereas "ns" indicates no statistical significance (at the 95% confidence level), assessed using a one-tailed Student's *t*-test.

A calibration curve was constructed by incubating CTSB-CLIP with increasing concentrations of CTSB protease for 30 min and then monitoring the CRISPR assay signal for an additional 2 h (Figure 4a). The limit of detection (LOD) was determined using the $3\sigma/m$ method. The LOD was found to be ~88 pM. In contrast, the LOD obtained using 100-times higher concentration of a CFP for CTSB was 3.4 nM, which is ~40-fold higher (Figure S25). The mechanism of action for CTSB-CFP is similar to that of 3CL-CFP, except that it uses 7-amino-4-methylcoumarin as the dye. Notably, the LOD of CTSB-CLIP is slightly higher compared to the lower end of the detection range of commonly used ELISA assays for CTSB (1.6–82 pM).[61–65] However, ELISA assays are unable to distinguish between active and inactive forms of the protein, require multiple steps, elevated temperatures (37 °C), and a total assay time of up to 5 h. Moreover, the LOD of CTSB-CLIP is well below the reported CTSB concentrations in the serum of colorectal cancer patients, which can reach up to 297 pM.[39]

To assess the selectivity of CTSB-CLIP, we tested its response to various proteases at 20 nM, including CTSB, 3CL, MMP7, thrombin (THR), CASP3, and trypsin (TRP). Bovine serum albumin (BSA) was used as an additional control to ensure nonspecific protein binding does not disrupt the locked hairpin-like structure of CLIPs. The results (Figures 4b and S7) confirmed that CTSB-CLIP is highly selective for CTSB compared to the other tested proteases and BSA.

CLIPs Detect Proteases in Complex Biological Matrices

We next explored the application of CLIPs in biologically relevant settings. We first assessed the stability of CLIPs in the presence of nucleases (Figure S26) and cell lysates (Figure S27). DNase I, which degrades both single- and double-stranded DNA was applied to 3CL-CLIP at varying concentrations. Our results (Figure S26) show that after 30 min of treatment, while the CLIP structure is degraded

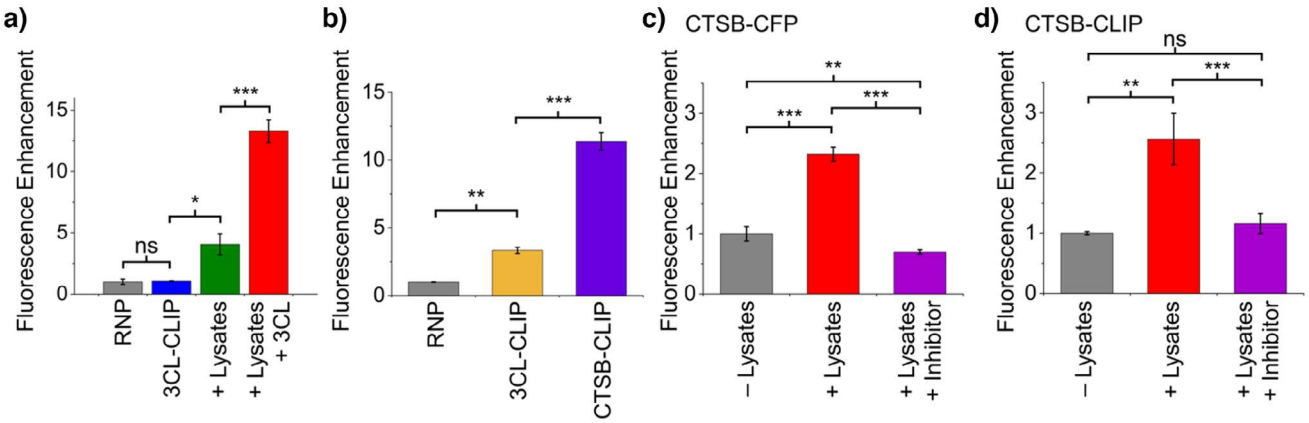

Figure 5. a) Detection of 1 μM 3CL protease spiked into NCI-H508 cell lysates using 3CL-CLIP. b) Activation of CTSB-CLIPs when treated with 15 μL of lysates from RKO cell line. 3CL-CLIP is used as a control. Fluorescence enhancement is defined as ratio of the fluorescence values of a sample to the fluorescence of the RNP complex. c) Signal generated when 100 nM CTSB-CFP is treated with 6 μL of RKO cell lysates in the presence and absence of a CTSB inhibitor. d) Signal generated when 1 nM CTSB-CLIP is treated with 6 μL of RKO cell lysates in the presence and absence of a CTSB inhibitor. *, **, and *** denote statistical significance at the 95%, 99%, and 99.9% confidence levels, respectively, whereas "ns" indicates no statistical significance (at the 95% confidence level), assessed using a one-tailed Student's *t*-test.

at high DNase I concentrations, it remains stable at DNase activity of 25 U L^{-1} or lower. This is more than double the activity of DNAse I in human serum (~10 U L^{-1}), demonstrating the robustness of the CLIP structure under relevant scenarios.[66] Similarly, CLIPs were found to show minimal degradation in cell lysates for up to 6 h (Figure S27).

We next investigated the functionality of CLIPs in complex biological media by testing them with cell lysates and 10% human serum. Specifically, we introduced 3CL protease into lysates from the NCI-H508 cell line, a type of colorectal cancer cell line that does not naturally produce 3CL protease. Any detection of signal in the absence of the spiked 3CL protease can be considered background noise. We observed that mixing the cell lysates with 3CL-CLIP resulted in some signal generation, which is likely from nonspecific cleavage of the probe or disruption of the locked structure due to the complex nature of the sample. However, when we added a spike of 1 μM 3CL protease to the lysates, the signal increased substantially, confirming that CLIPs are still effective in detecting target active proteases within a complex cell lysate solution (Figure 5a). Similar results were observed in 10% human serum (Figure S28). Although the addition of 3CL-CLIP to 10% serum produced a higher background signal compared to buffer, the signal increased significantly upon adding 1 μM 3CL protease, demonstrating that the probe remains effective in this medium. These findings align with control experiments using 3CL-CFP, a probe with a similar peptide sequence to 3CL-CLIP, which also exhibited background signal in 10% human serum (Figure S28).

We further explored whether CLIPs could detect endogenous proteases in biological samples, choosing CTSB as the target protease due to its known dysregulation in colorectal cancer.[60,67–69] To ensure the probe's applicability across different cell types, we investigated four different colon cancer cell lines—HT29, NCI-H508, RKO, and SW-620 (Figures S29–S31). The lysates were incubated with CTSB-CLIP and assayed using CRISPR (Figures 5b–d and S29). To assess background signal, 3CL-CLIPs were used. CTSB-CLIPs treated with cell lysates showed up to a 21-fold increase in fluorescence relative to the fluorescence of the RNP alone within 30 min (Figures 5b and S29). Although some background fluorescence was observed with the 3CL-CLIP, the signal from CTSB-CLIP was substantially higher. Using the most responsive cell line, SW-620, the probe successfully detected active CTSB from as few as 6,000 cells (Figure S30). For context, this number is on the lower end of cell quantities typically extracted during fine needle biopsies in cancer diagnostics.[70] We validated the presence of CTSB in the cell lysates using a CTSB-specific CFP (Figures 5c and Figure S31). Additionally, we introduced a commercial CTSB inhibitor to the RKO lysates, which led to a reduction in fluorescence signals from both the CTSB-CFP and CTSB-CLIP (Figure 5c,d). These experiments confirm the specificity of our detection method for active CTSB in complex biological samples.

Conclusion

In conclusion, CLIPs represent a powerful new class of activity-based sensors, offering a simple, rapid, room temperature method to detect proteases. They outperform commercial probes even at 100 times lower concentrations due to the incorporation of DNA, which serves as a handle for signal amplification. The DNA handle not only enhances detection capabilities beyond those of previous peptide beacons[71,72] but also simplifies the detection process relative to nanoparticle-based approaches. Unlike earlier nucleic acid-based strategies, CLIPs do not require complex synthetic biology or separation of "free" DNA from intact probes, making the detection one-pot and rapid, with overall assay times as fast as 35 min (30 min protease incubation followed by 5 min CRISPR assay). CLIPs also eliminate the need for sophisticated equipment by utilizing commonly available plate readers for readouts. Moreover,

adjustments to the initiator and blocking strands could optimize CLIP performance in various conditions, such as at elevated temperatures or different ionic strengths. The modular nature of the probe allows for detecting a variety of proteases in complex matrices simply by changing the peptide sequence. Importantly, the unique structure of CLIPs ensures that they only activate CRISPR in the presence of a target, providing a solid foundation for detecting not only proteases but also potentially other disease-relevant enzymes with cleavable substrates. As the detection is based on irreversible peptide cleavage, each probe is single-use. Although CRISPR-mediated signaling is currently employed to detect the activated initiator strand, integration of other DNA detection techniques could further boost sensitivity, potentially achieving detection at the single-cell level. Taken together, the flexibility, sensitivity, and specificity of CLIPs establish them as a versatile and promising approach for activity-based sensing, making them a valuable addition to the MB toolbox.

Supporting Information

DNA and peptide sequences used in this study; details of materials and methods, synthesis, characterization, and further validation of all CLIP structures; further hypothesis and results with blocked CRISPR-Cas12a systems; melting temperature analysis and design of CLIPs, further protease and cell lysate results with CLIPs. The authors have cited additional references within the Supporting Information.[52,60,66,67,73–78]

Acknowledgements

This work is supported by start-up funds from The University of Texas at Austin, IRG-21–135–01-IRG from the American Cancer Society, the National Science Foundation (NSF CHE 2404334), Grant #2024–77398 from the Packard Foundation, and the Cancer Prevention and Research Institute of Texas (CPRIT) Grant RR 160093. M.L.C. was supported by an undergraduate research fellowship from the Office of Undergraduate Research at UT Austin. B.J.A. was supported by an NSF-REU. Images were created using Biorender.com, Avogadro, PyMOL, and OriginPro 2024.

Conflict of Interests

The authors declare no conflict of interest.

Data Availability Statement

The data that support the findings of this study are available from the corresponding author upon reasonable request.

Keywords: Activity-based sensing · Detection · DNA · Nanostructures · Protease

[1] S. Tyagi, F. R. Kramer, *Nat. Biotechnol.* **1996**, *14*, 303–308.
[2] K. Wang, Z. Tang, C. J. Yang, Y. Kim, X. Fang, W. Li, Y. Wu, C. D. Medley, Z. Cao, J. Li, P. Colon, H. Lin, W. Tan, *Angew. Chem. Int. Ed.* **2009**, *48*, 856–870.
[3] S. Tyagi, D. P. Bratu, F. R. Kramer, *Nat. Biotechnol.* **1998**, *16*, 49–53.
[4] J. Zheng, R. Yang, M. Shi, C. Wu, X. Fang, Y. Li, J. Li, W. Tan, *Chem. Soc. Rev.* **2015**, *44*, 3036–3055.
[5] C. Sheng, J. Zhao, Z. Di, Y. Huang, Y. Zhao, L. Li, *Nat. Biomed. Eng.* **2022**, *6*, 1074–1084.
[6] A. S. Piatek, S. Tyagi, A. C. Pol, A. Telenti, L. P. Miller, F. R. Kramer, D. Alland, *Nat. Biotechnol.* **1998**, *16*, 359–363.
[7] S. Cai, T. Pataillot-Meakin, A. Shibakawa, R. Ren, C. L. Bevan, S. Ladame, A. P. Ivanov, J. B. Edel, *Nat. Commun.* **2021**, *12*, 3515.
[8] S. P. Tripathy, M. Ponnapati, S. Bhat, J. Jacobson, P. Chatterjee, *Sci. Adv.* **2022**, *8*, eabn2378.
[9] J. Yang, Y. Quan, Y. Ouyang, K. O. Tan, R. T. Weber, R. G. Griffin, R. T. Raines, *Biomacromolecules* **2024**, *25*, 6773–6779.
[10] A. Dhar, I. Ahmed, S. Mallick, S. Roy, *ChemBioChem* **2020**, *21*, 2121–2125.
[11] M. Okochi, T. Sugita, M. Tanaka, H. Honda, *RSC Adv.* **2015**, *5*, 91988–91992.
[12] S. Thurley, L. Röglin, O. Seitz, *J. Am. Chem. Soc.* **2007**, *129*, 12693–12695.
[13] C. Mueller, T. N. Grossmann, *Angew. Chem. Int. Ed.* **2018**, *57*, 17079–17083.
[14] C. J. Chang, T. D. James, E. J. New, B. Z. Tang, *Acc. Chem. Res.* **2020**, *53*, 1.
[15] A. P. Soleimany, S. N. Bhatia, *Trends Mol. Med.* **2020**, *26*, 450–468.
[16] E. J. Kwon, J. S. Dudani, S. N. Bhatia, *Nat. Biomed. Eng.* **2017**, *1*, 1–10.
[17] M. M. Kaminski, O. O. Abudayyeh, J. S. Gootenberg, F. Zhang, J. J. Collins, *Nat. Biomed. Eng.* **2021**, *5*, 643–656.
[18] D. Samanta, S. B. Ebrahimi, N. Ramani, C. A. Mirkin, *J. Am. Chem. Soc.* **2022**, *144*, 16310–16315.
[19] R. Chowdhry, S. Z. Lu, S. Lee, S. Godhulayyagari, S. B. Ebrahimi, D. Samanta, *Trends Biotechnol.* **2023**, *41*, 1549–1564.
[20] J. S. Chen, E. Ma, L. B. Harrington, M. D. Costa, X. Tian, J. M. Palefsky, J. A. Doudna, *Science* **2018**, *360*, 436–439.
[21] M. J. Kellner, J. Koob, J. S. Gootenberg, O. O. Abudayyeh, F. Zhang, *Nat. Protoc.* **2019**, *14*, 2986–3012.
[22] A. P. Amini, J. D. Kirkpatrick, C. S. Wang, A. M. Jaeger, S. Su, S. Naranjo, Q. Zhong, C. M. Cabana, T. Jacks, S. N. Bhatia, *Nat. Commun.* **2022**, *13*, 5745.
[23] J. S. Dudani, M. Ibrahim, J. Kirkpatrick, A. D. Warren, S. N. Bhatia, *Proc. Natl. Acad. Sci. USA* **2018**, *115*, 8954–8959.
[24] M. Anahtar, L. W. Chan, H. Ko, A. Rao, A. P. Soleimany, P. Khatri, S. N. Bhatia, *Proc. Natl. Acad. Sci. USA* **2022**, *119*, e2121778119.
[25] M. F. Schmidt, Z. Y. Gan, D. Komander, G. Dewson, *Cell Death Differ.* **2021**, *28*, 570–590.
[26] Q. Zheng, T. Huang, L. Zhang, Y. Zhou, H. Luo, H. Xu, X. Wang, *Front. Aging Neurosci.* **2016**, *8*, 303.
[27] C. T. N. Pham, *Nat. Rev. Immunol.* **2006**, *6*, 541–550.
[28] C.-L. Liu, J. Guo, X. Zhang, G. K. Sukhova, P. Libby, G.-P. Shi, *Nat. Rev. Cardiol.* **2018**, *15*, 351–370.
[29] J. A. Kudryashev, L. E. Waggoner, H. T. Leng, N. H. Mininni, E. J. Kwon, *ACS Sens.* **2020**, *5*, 686–692.
[30] V. Suresh, K. Byers, U. C. Rajesh, F. Caiazza, G. Zhu, C. S. Craik, K. Kirkwood, V. J. Davisson, D. A. Sheik, *Diagnostics* **2022**, *12*, 1343.
[31] Q. D. Mac, D. V. Mathews, J. A. Kahla, C. M. Stoffers, O. M. Delmas, B. A. Holt, A. B. Adams, G. A. Kwong, *Nat. Biomed. Eng.* **2019**, *3*, 281–291.

[32] S. S. Liew, Z. Zeng, P. Cheng, S. He, C. Zhang, K. Pu, *J. Am. Chem. Soc.* **2021**, *143*, 18827–18831.
[33] Y. Chen, P. Pei, Y. Yang, H. Zhang, F. Zhang, *Angew. Chem. Int. Ed.* **2023**, *62*, e202301696.
[34] J. J. Yim, S. Harmsen, K. Flisikowski, T. Flisikowska, H. Namkoong, M. Garland, N. S. van den Berg, J. G. Vilches-Moure, A. Schnieke, D. Saur, S. Glasl, D. Gorpas, A. Habtezion, V. Ntziachristos, C. H. Contag, S. S. Gambhir, M. Bogyo, S. Rogalla, *Proc. Natl. Acad. Sci. USA* **2021**, *118*, e2008072118.
[35] C. Xu, K. Pu, *Nat. Rev. Bioeng.* **2024**, *2*, 425–441.
[36] L. E. Sanman, M. Bogyo, *Annu. Rev. Biochem.* **2014**, *83*, 249–273.
[37] A. Saghatelian, N. Jessani, A. Joseph, M. Humphrey, B. F. Cravatt, *Proc. Natl. Acad. Sci. USA* **2004**, *101*, 10000–10005.
[38] R. Xing, A. K. Addington, R. W. Mason, *Biochem. J.* **1998**, *332*, 499–505.
[39] J. Kos, H. J. Nielsen, M. Krasovec, I. J. Christensen, N. Cimerman, R. W. Stephens, N. Brünner, *Clin. Cancer Res.* **1998**, *4*, 1511–1516.
[40] M. Vočka, D. Langer, V. Fryba, J. Petrtyl, T. Hanus, M. Kalousova, T. Zima, L. Petruzelka, *Int. J. Biol. Markers* **2019**, *34*, 292–301.
[41] S. Pandit, M. Duchow, W. Chao, A. Capasso, D. Samanta, *Angew. Chem. Int. Ed.* **2023**, *63*, e202310964.
[42] L. Hao, R. T. Zhao, N. L. Welch, E. K. W. Tan, Q. Zhong, N. S. Harzallah, C. Ngambenjawong, H. Ko, H. E. Fleming, P. C. Sabeti, S. N. Bhatia, *Nat. Nanotechnol.* **2023**, *18*, 798–807.
[43] F. Liu, M. Yang, W. Song, X. Luo, R. Tang, Z. Duan, W. Kang, S. Xie, Q. Liu, C. Lei, Y. Huang, Z. Nie, S. Yao, *Chem. Sci.* **2020**, *11*, 2993–2998.
[44] S. Xie, C. Zhu, L. Yang, H. Li, H. Zhu, Z. Nie, C. Lei, *Anal. Chem.* **2023**, *95*, 10728–10735.
[45] X. Luo, J. Zhao, X. Xie, F. Liu, P. Zeng, C. Lei, Z. Nie, *Anal. Chem.* **2020**, *92*, 16314–16321.
[46] Q. Zhong, E. K. W. Tan, C. Martin-Alonso, T. Parisi, L. Hao, J. D. Kirkpatrick, T. Fadel, H. E. Fleming, T. Jacks, S. N. Bhatia, *Sci. Adv.* **2024**, *10*, eadj9591.
[47] Z. Jin, C. Ling, Y. Li, J. Zhou, K. Li, W. Yim, J. Yeung, Y.-C. Chang, T. He, Y. Cheng, P. Fajtová, M. Retout, A. J. O'Donoghue, J. V. Jokerst, *Nano Lett.* **2022**, *22*, 8932–8940.
[48] E. Heilmann, F. Costacurta, S. A. Moghadasi, C. Ye, M. Pavan, D. Bassani, A. Volland, C. Ascher, A. K. H. Weiss, D. Bante, R. S. Harris, S. Moro, B. Rupp, L. Martinez-Sobrido, D. von Laer, *Sci. Transl. Med.* **2023**, *15*, eabq7360.
[49] Z. Jin, Y. Mantri, M. Retout, Y. Cheng, J. Zhou, A. Jorns, P. Fajtova, W. Yim, C. Moore, M. Xu, M. N. Creyer, R. M. Borum, J. Zhou, Z. Wu, T. He, W. F. Penny, A. J. O'Donoghue, J. V. Jokerst, *Angew. Chem. Int. Ed.* **2022**, *61*, e202112995.
[50] M. Retout, Y. Mantri, Z. Jin, J. Zhou, G. Noël, B. Donovan, W. Yim, J. V. Jokerst, *ACS Nano* **2022**, *16*, 6165–6175.
[51] "3C. L. Protease, MBP-tagged (SARS-CoV-2) Assay Kit", can be found under https://bpsbioscience.com/3cl-protease-sars-cov-2-assay-kit-79955 (accessed: October 2024).
[52] T. MacCulloch, A. Novacek, N. Stephanopoulos, *Chem. Commun.* **2022**, *58*, 4044–4047.
[53] S. K. Albert, S. Lee, P. Durai, X. Hu, B. Jeong, K. Park, S.-J. Park, *Small* **2021**, *17*, 2006110.
[54] B. Bian, S. Mongrain, S. Cagnol, M.-J. Langlois, J. Boulanger, G. Bernatchez, J. C. Carrier, F. Boudreau, N. Rivard, *Mol. Carcinog.* **2016**, *55*, 671–687.
[55] H. Shantha Kumara, H. Miyagaki, S. A. Herath, E. Pettke, X. Yan, V. Cekic, R. L. Whelan, *World J. Gastrointest. Oncol.* **2021**, *13*, 879–892.
[56] S. Yuan, L. Lin, R.-H. Gan, L. Huang, X. Wu, Y. Zhao, B. Su, D. Zheng, Y.-G. Lu, *BMC Cancer* **2020**, *20*, 33.
[57] C. S. Gondi, J. S. Rao, *Expert Opin. Ther. Targets* **2013**, *17*, 281–291.
[58] N. Aggarwal, B. F. Sloane, *Proteomics Clin. Appl.* **2014**, *8*, 427–437.
[59] A. G. Porter, R. U. Jänicke, *Cell Death Differ.* **1999**, *6*, 99–104.
[60] A. Chan, Y. Baba, K. Shima, K. Nosho, D. Chung, K. Hung, U. Mahmood, K. Madden, K. Poss, A. Ranieri, D. S. Shue, R. Kucherlapati, C. Fuchs, S. Ogino, *Cancer Epidemiol. Biomarkers Prev.* **2010**, *19*, 2777–2785.
[61] LSBio, "Human CTSB /Cathepsin B (Sandwich ELISA) ELISA Kit", can be found under https://www.lsbio.com/elisakits/human-ctsb-cathepsin-b-sandwich-elisa-elisa-kit-ls-f1026/1026 (accessed January 2025).
[62] A. F. G. Scientific, "Human cathepsin B (CTSB) ELISA Kit", can be found under https://www.afgsci.com/product/human-cathepsin-b-ctsb-elisa-kit/ (accessed January 2025).
[63] Bio-Techne, "Human Total Cathepsin B DuoSet ELISA", can be found under https://www.rndsystems.com/products/human-total-cathepsin-b-duoset-elisa_dy2176 (accessed January 2025).
[64] M. S. E. Supplies, "Human CTSB(Cathepsin B) ELISA Kit", can be found under https://www.msesupplies.com/products/human-ctsbcathepsin-b-elisa-kit (accessed January 2025).
[65] Antibodies.com, "Human Cathepsin B ELISA Kit", can be found under https://www.antibodies.com/catalog/elisa-kits/human-cathepsin-b-elisa-kit-a310662 (accessed January 2025).
[66] Y. Kawai, M. Yoshida, K. Arakawa, T. Kumamoto, N. Morikawa, K. Masamura, H. Tada, S. Ito, H. Hoshizaki, S. Oshima, K. Taniguchi, H. Terasawa, I. Miyamori, K. Kishi, T. Yasuda, *Circulation* **2004**, *109*, 2398–2400.
[67] E. Campo, J. Muñoz, R. Miquel, A. Palacín, A. Cardesa, B. F. Sloane, M. Emmert-Buck, *Am. J. Pathol.* **1994**, *145*, 301–9.
[68] K. Hirai, M. Yokoyama, G. Asano, S. Tanaka, *Hum. Pathol.* **1999**, *30*, 680–686.
[69] K. E. Hung, M. A. Maricevich, L. G. Richard, W. Y. Chen, M. P. Richardson, A. Kunin, R. T. Bronson, U. Mahmood, R. Kucherlapati, *Proc. Natl. Acad. Sci. USA* **2010**, *107*, 1565–1570.
[70] P. H. Lizotte, R. E. Jones, L. Keogh, E. Ivanova, H. Liu, M. M. Awad, P. S. Hammerman, R. R. Gill, W. G. Richards, D. A. Barbie, A. J. Bass, R. Bueno, J. M. English, M. Bittinger, K.-K. Wong, *Sci. Rep.* **2016**, *6*, 31745.
[71] M. Fischbach, U. Resch-Genger, O. Seitz, *Angew. Chem. Int. Ed.* **2014**, *53*, 11955–11959.
[72] I. Y. Lee, P. Tantisirivat, L. E. Edgington-Mitchell, *ACS.Bio. Med. Chem. Au* **2023**, *3*, 295–304.
[73] M. Abdulla, M.-A. Valli-Mohammed, K. Al-Khayal, A. A. Shkieh, A. Zubaidi, R. Ahmad, K. Al-saleh, O. Al-Obeed, J. McKerrow, *Oncol. Rep.* **2017**, *37*, 3175–3180.
[74] L. G. M. Hazen, F. Bleeker, B. Lauritzen, S. Bahns, J. Song, A. Jonker, B. V. Driel, H. Lyon, U. Hansen, A. Köhler, C. Noorden, *J. Histochem. Cytochem.* **2000**, *48*, 1421–1430.
[75] S. R. K. Ainavarapu, J. Brujić, H. H. Huang, A. P. Wiita, H. Lu, L. Li, K. A. Walther, M. Carrion-Vazquez, H. Li, J. M. Fernandez, *Biophys. J.* **2007**, *92*, 225–233.
[76] J. Ambia-Garrido, A. Vainrub, B. M. Pettitt, *Comput. Phys. Commun.* **2010**, *181*, 2001–2007.
[77] A. N. Rao, D. W. Grainger, *Biomater. Sci.* **2014**, *2*, 436–471.
[78] Q. Chi, G. Wang, J. Jiang, *Phys. A Stat. Mech. Appl.* **2013**, *392*, 1072–1079.

Manuscript received: January 08, 2025
Revised manuscript received: April 06, 2025
Accepted manuscript online: April 08, 2025
Version of record online: ■■, ■■

Research Article

DNA Nanotechnology

D. M. Snider, M. L. Coffin, B. J. Armijo, R. Khetan, M. W. Duchow, A. Capasso, D. Samanta* **e202500649**

Conformationally Locked Peptide–DNA Nanostructures for CRISPR-Amplified Activity-Based Sensing

We report a new class of chemical probes, termed cleavable, locked initiator probes (CLIPs). CLIPs are peptide–DNA nanostructures resembling molecular beacons but enable activity-based CRISPR-amplified molecular sensing. CLIPs detect various disease-relevant proteases, yield superior sensitivity compared to commercial probes, and enable the monitoring of active proteases in colorectal cancer cell lysates.

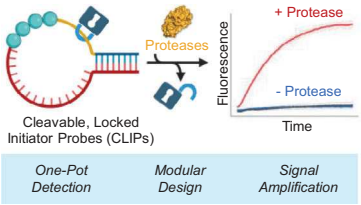

Supporting Information

Conformationally Locked Peptide-DNA Nanostructures for CRISPR-Amplified Activity-Based Sensing

Dylan M. Snider,[a] Mackenzie L. Coffin,[a] Brian J. Armijo,[a] Ryan Khetan,[a] Mark W. Duchow,[b] Anna Capasso,[b] and Devleena Samanta[a,c,d,*]

[a]Department of Chemistry, The University of Texas at Austin, 105 E 24th St., Austin, TX 78712.

[b]Department of Oncology, Dell Medical School, The University of Texas at Austin, 1601 Trinity St., Austin, TX 78712.

[c]Livestrong Cancer Institutes, Dell Medical School, The University of Texas at Austin, 1601 Trinity St., Austin, TX 78712.

[d]Texas Materials Institute, The University of Texas at Austin, 2501 Speedway, Austin, TX 78712.

*E-mail: dsamanta@utexas.edu

Table of Contents

1 Peptide and Nucleic Acid Sequences Used in This Study

Table S1. Peptide sequences used in this study.

Name	Sequences (N-C)	Expected Molecular Weight (Da)	Observed Molecular Weight *(m/z)*
Pep-3CL	CSAVLQSGFK(N_3)	1,139	1,279
Pep-MMP7	CKRWLALPGK(N_3)	1,370	1,412
Pep-CTSB	CGAARRGGGK(N_3)	1,032	1,172
Pep-CASP3	CADEVDGGGK(N_3)	1,049	998

Table S2. Nucleic acid sequences used in this study.

Name	Sequences (5'-3')	Expected Molecular Weight (Da)	Observed Molecular Weight *(m/z)*	Extinction Coefficient at 260 nm ($Lmol^{-1}cm^{-1}$)
Initiator DNA	DBCO-TEG TTT T**GT GCT GCC ATA TCT ACT TCA**	7,830	7,997	223,900
Blocking DNA	TGA AGT AG T(DBCO)	3,546	3,527	95,600
Quencher-labeled Initiator DNA	DBCO-TEG TTT T**GT GCT GCC ATA TCT ACT TCA** BHQ	8,312	8,446	223,900
Dye-labeled Blocking DNA	Cy5 TGA AGT AG T(DBCO)	3,780	3,761	97,100
DNA Hairpin 30-8	TGA AGT AGT TTT TTT TTT TTT TTT TTT TTT TTT TTT TTT TTT **GTG CTG CCA TAT CTA CTT CA**	18,921	18,929	545,800
DNA Hairpin 10-8	TGA AGT AGT TTT TTT TTT TTT T**GT GCT GCC ATA TCT ACT TCA**	12,837	12,971	383,800
24-nt Blocking DNA	TGA AGT AGA TAT GGC AGC ACA AAA	7,443	7,465	255,700
16-nt Blocking DNA	ATA TGG CAG CAC AAA A	4,907	4,966	170,300
gRNA	rUrArArUrUrUrCrUrArCrUrArArGr UrGrUrArGrArUrUrGrArArGrUrAr GrArUrArUrGrGrCrArGrCrArC	13,160	13,232	432,100

*Sequences that are **bolded** are complementary to the underlined sequence in the gRNA.

2 Size Comparison of CRISPR Components and CLIPs

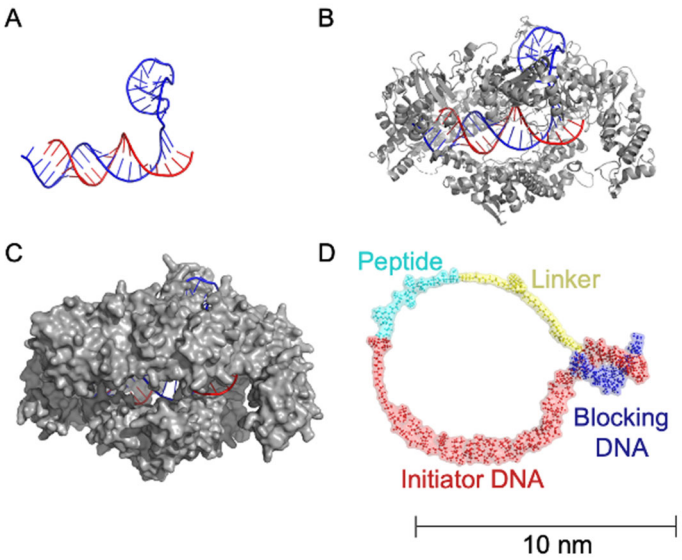

Figure S1. (A) Structure of a 40-nt gRNA hybridized to a 20-nt DNA initiator, (B) Cartoon representation of the structure of the gRNA-DNA hybrid bound to a CRISPR-Cas12a enzyme, (C) Surface representation of the structure of the gRNA-DNA hybrid bound to a CRISPR-Cas12a enzyme. These structures are modeled using protein data bank entry 6I1L. (D) Expected molecular structure of 3CL-CLIP.

3 Hypothesized Interaction Between CLIPs and Cleaved CLIPs with CRISPR-RNP

We hypothesized that the hairpin-like conformation of CLIPs prevents the activation of CRISPR-Cas12a ribonucleoprotein (RNP) complexes until cleaved by an active protease. Uncleaved CLIPs should not activate the CRISPR-Cas12a RNP for two reasons: 1) the Blocking DNA prevents the Initiator DNA from hybridizing with the gRNA in the RNP, and 2) Steric hindrance caused by the non-DNA portion in the loop region of the CLIP obstructs the enzyme from accessing the Initiator DNA.

Once the CLIPs are cleaved by target proteases, the newly liberated single-stranded Initiator DNA is free from these impediments and activates the CRISPR-Cas12a. This activated CRISPR-Cas12a then exhibits non-specific endonuclease activity, allowing it to catalytically cleave DNase Alert reporters, which results in a significant increase in fluorescence. This fluorescence is then measured as a proxy for the protease's activity.

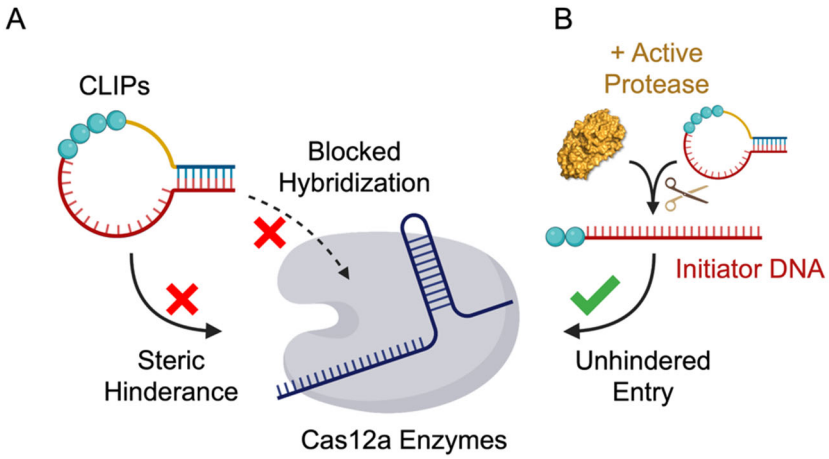

Figure S2. Hypothesized interaction between CRISPR-Cas12a RNP and (A) intact CLIPs, as well as (B) protease-treated CLIPs.

4 Materials and Methods

4.1 Buffers Commonly Used in the Study

Below is a list of buffers commonly used in this study, along with their respective concentrations. Composition is excluded for buffers that were purchased from commercial vendors.

CRISPR Buffer	40 mM Tris-HCl pH 7.5 100 mM sodium chloride (salt purchased from Fisher Bioreagents, Cat. No: BP358-212) 40 mM magnesium chloride (salt purchased from Fisher Bioreagents, Cat. No: M33-500)
3CL Buffer	BPS Bioscience, Cat. No: 79956
CTSB Buffer	1X DPBS 15 mM DTT 2 mM EDTA
MMP7 Buffer	1X DPBS 15 mM DTT
CASP3 Buffer	1X PBS
1 M Tris-HCl pH 7.5	Invitrogen, Cat. No: 15567-027
10X PBS	Thermo Fisher Scientific, pH 7.4, Cat. No: J62036.K2
10X TBE	Fisher BioReagents, Tris-Borate-EDTA 10X, Cat. No: BP1333-4
1X DPBS	Sigma-Aldrich, Cat. No: D8537

4.2 Synthesis, Purification, and Characterization of DNA

DNA sequences were synthesized at the 1 µmol scale through solid-phase DNA synthesis using a MerMade 6 automated DNA synthesizer (LGC Biosearch Technologies, Alexandria MN 56308). DNA was synthesized on a solid support, specifically controlled pore glass (CPG) beads. Depending on the sequence, either universal CPG (Glen Research, UnySupport CPG-1000, Cat. No: 20-5040) or 3’ black hole quencher CPG beads (3'-BHQ-2 CPG, Cat. No: 20-5932-01) were used.

All DNA phosphoramidites and materials required for solid-phase DNA synthesis were purchased from Glen Research: (dA-CE phosphoramidite, Cat. No: 10-1000-10), (dC-CE phosphoramidite, Cat. No: 10-1010-10), (dT-CE phosphoramidite, Cat. No: 10-1030-10), (DMF-dG phosphoramidite, Cat. No: 10-29-10), (DBCO-dT-CE phosphoramidite, Cat. No: 10-1539-95), (5’-DBCO-TEG Phosphoramidite, Cat. No: 10-1941-90), (Cyanine 5 Phosphoramidite, 10-5915-95), (0.25M 5-Ethylthio-1H-Tetrazole (ETT) in Anhydrous Acetonitrile, Cat. No: 30-3140-52), (3% TCA/DCM, Cat. No: 40-4140-57), (0.02M Iodine in Tetrahydrofuran/Pyridine/Water (70:20:10), Cat. No: 40-4330-52), (Anhydrous acetonitrile, 40-4050-57). Sequences made this way include Initiator DNA, Blocking DNA, Quencher-labeled Initiator DNA, and Dye-labeled Blocking DNA. Sequences purchased from Integrated DNA Technologies include DNA Hairpin 30-8, DNA Hairpin 10-8, 24-nt DNA Blocking DNA, and 16-nt Blocking DNA.

After synthesis the beads were treated with 1 mL (per µmol of DNA) of a 30% ammonium hydroxide solution (Sigma-Aldrich, Cat. No: 221228-100ML-A) for 17 h at room temperature (RT). The solution was then evaporated under an airstream at RT (for ~10 min). 1 mL water was then added, and the beads were separated from free DNA in solution using a syringe filter and then purified.

Unmodified DNA sequences (in which the desired full-length sequences contain a 4,4'-dimethoxytrityl group) or those containing 5’ DBCO-TEG groups, were purified using a Glen-Pak cartridge (Glen Research, Glen-Pak DNA purification cartridge, Cat. No: 60-5200) following the manufacturer’s recommended protocol.

DNA containing a 3’DBCO-dT group, specifically the Blocking DNA, was purified through high performance liquid chromatography (HPLC) using a Vanquish HPLC (Thermo Fisher Scientific, Vanquish Core HPLC Systems, Cat. No: VQ-CORE-BIN-01). Buffer A was 30 mM triethylammonium acetate (prepared by mixing 1:1 molar equivalents of triethylamine (Fisher Scientific, Triethylamine (Reagent), Cat. No: O4885-1) and glacial acetic acid (Fisher Scientific, Acetic Acid, Glacial (TraceMetal Grade), Cat. No: A507-P500) over ice to pH 7 with 3% acetonitrile (ACN) in water, while buffer B was 100% acetonitrile. The method followed a gradient increase from 10% to 35% buffer B over 80 min,

a ramp to 100% buffer B over 5 min followed by 5 min of 100% buffer B, a ramp down to 5% buffer B over five min followed by 5% buffer B for 5 min. Separation was monitored through UV-Vis peaks at 260 nm and 310 nm for DNA and DBCO respectively. All peaks were collected, lyophilized, and redissolved in water for characterization.

4.3 Synthesis, Purification, and Characterization of Peptides

All peptides were synthesized in-house using standard Fmoc-based solid-phase synthesis on a 0.1 mmol scale. Synthesis was conducted using Rink Amide AM resin 100-200 mesh (Sigma-Aldrich, Cat. No: 183599-10-2) inside a fritted 6 mL syringe. The resin was initially prepared by washing with 5 mL of dimethylformamide (DMF) (Millipore Sigma, N,N-Dimethylformamide, Cat. No: 270547), for 15 min.

Peptides were synthesized by adding amino acids sequentially in the following cycle: (1) the functionalized resin was washed with 5 mL of DMF. (2) The sample was deprotected using 5 mL of 20% piperidine (Millipore Sigma, Piperidine Solution 20% in DMF, Cat. No: 80645) for 5 min and the piperidine was removed through the syringe. Then, the same reagent was added and the deprotection step was continued for another 20 min. Piperidine was washed from the syringe using DMF until the piperidine smell disappeared. (3) The amino acid (0.25 mmol) was then added to the resin along with coupling reagents (2.5 equiv. HOBt, 2.5 equiv. DIC) in 3 mL DMF. This coupling was run for 2 h at RT but couplings involving Fmoc Lys (N3)-OH (AnaSpec.Inc, Cat. No: AS-53100-F1) were allowed to run overnight. This cycle was followed until all amino acids had been added and then deprotected using the earlier mentioned procedure.

Peptides were cleaved from the resin surface using 1 mL of a cocktail solution of trifluoroacetic acid (TFA) (Sigma-Aldrich, Cat. No: 302031-100ML), H_2O, and triisopropylsilane (TCI, Cat. No: T1533) in a volumetric ratio of 95:2.5:2.5, shaking at RT for 2 h. Taking 100 µL portions of this solution and adding them dropwise into chilled diethyl ether (Millipore Sigma, Diethyl ethyl, Cat. No:296082) the peptide was precipitated and recovered using centrifugation at 15,000 rpm for 3 min. This was repeated until all the solution was collected and was further washed using this method using fresh chilled diethyl ether. The peptide was then stored dry at 4 °C until further use.

4.4 Synthesis, Purification, and Characterization of CLIPs

CLIPs were synthesized sequentially as per the reaction scheme below:

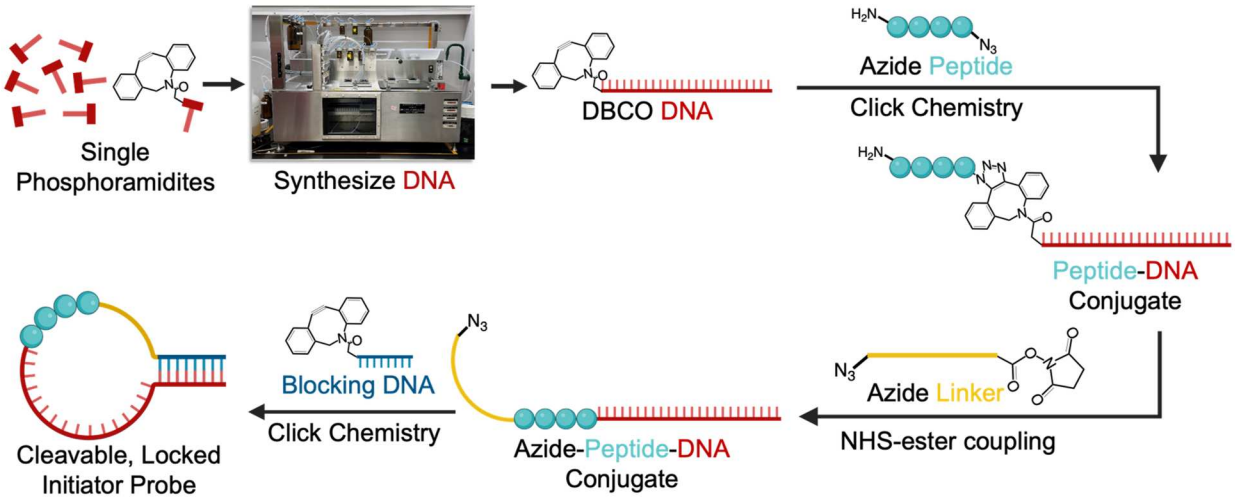

Figure S3. Scheme for synthesizing CLIPs.

First, peptide-DNA conjugates were synthesized through copper free click chemistry using azido-peptides and dibenzocyclooctyne (DBCO) modified DNA. The peptides used were (Pep-3CL, Pep-MMP7, Pep-CTSB, and Pep-CASP3 from **Table S1**), and the DBCO-DNA was the Initiator DNA as seen in **Table S2**. Peptides were reacted with DNA at a 5:1 molar ratio in 1X phosphate-buffered saline (PBS) (Thermo Scientific, pH 7.4, Cat. No: J62036.K2) with shaking at RT overnight. 1 µmol of Initiator DNA was used and reacted at a concentration of ~ 600 µM. The reaction was monitored for completion via UV-Vis. Disappearance of the DBCO's characteristic 310 nm peak indicated that all DNA had been reacted. The solution was then washed using a 3 kDa centrifuge filter (Amicon Ultra, UFC500396) five times with 0.5 mL of ultrapure water and characterized via UV-Vis.

Free peptides were removed from the peptide-DNA conjugates using a Macro-Prep DEAE weak anionic exchange resin (Bio-Rad, Cat. No: 158-0020). Into a fritted 6 mL syringe, 2 mL of the DEAE resin was loaded and washed with 5 column volumes of ultrapure water. Before applying the sample, tris (2-carboxyethyl) phosphine hydrochloride (TCEP) (Sigma-Aldrich, Tris(2-carboxyethyl) phosphine hydrochloride, Cat. No: C4706) was added to the sample at a final concentration of 10 mM and allowed to shake at 1500 RPM (Benchmark, Multi-Therm Heating Shaker, Cat. No: H5000-H) for 15 min to break any disulfide bonds between the peptides. The entirety of the sample was then applied to the DEAE at a flow rate of 1 drop per s, washed with 5 column volumes of water, then of 0.3 M NaCl, and peptide-DNA conjugates were then eluted with 1 mL of 1 M sodium chloride (NaCl) (Fisher Bioreagents, Sodium Chloride, BP358-212). The elution of the peptide-DNA conjugate was monitored using UV-Vis utilizing DNA's characteristic absorbance at 260 nm. No significant DNA peaks were seen in water or 0.3 M NaCl washes. However, when 1 mL of 1 M NaCl was used, the peptide-DNA conjugate could be recovered (~50%). Further washing with additional 1 M NaCl or higher concentrations did not yield additional DNA. The sample was then washed using a 3 kDa centrifuge filter five times with 0.5 mL of ultrapure water and peptide-DNA conjugate was characterized via UV-Vis, MALDI-MS, and gel electrophoresis.

Next, an azido PEG linker was installed on the peptide-DNA conjugate. These linker-peptide-DNAs were synthesized through NHS-ester conjugation between the peptide-DNA conjugate and NHS-PEG_4-Azide (Thermo Fisher, Cat. No: 26130). Before reacting, the peptide-DNAs were treated with TCEP at a final concentration of 10 mM shaking for 15 min. NHS-ester conjugation was carried out using 0.5 µmol of the peptide-DNAs and a 150-molar excess of the NHS-PEG_4-Azides in 2 mL of sodium bicarbonate (Fisher Bioreagents, Sodium Bicarbonate, Cat. No: BP328-500) with shaking at RT overnight. The sample was then washed using a 3 kDa centrifuge filter five times with 0.5 mL of ultrapure water and final conjugate was characterized via UV-Vis. Final yield was on average ~85%.

The final CLIP structure (i.e. the DNA-peptide-DNA triblock) was synthesized by reacting linker-peptide-DNAs with Blocking DNA using copper free click chemistry. 0.1 µmol of the linker-peptide-DNA was conjugated to the Blocking DNA (5:1 molar excess of Blocking DNA relative to linker-peptide-DNA) in 0.1 M NaCl PBS with shaking at 1500 RPM at RT for 16-48 h. The sample was then washed using a 3 kDa centrifuge filter ten times with 0.5 mL of ultrapure water and final conjugate was characterized via UV-Vis, MALDI-MS, and gel electrophoresis.

Purification of CLIPs was accomplished using HPLC separation. Buffer A was 30 mM triethylammonium acetate buffer pH 7 and 3% acetonitrile (ACN) in water, while buffer B was 100% ACN. The method followed a gradient increase from 10% to 25% buffer B over 80 min, a ramp to 100% buffer B over 5 min followed by 5 min of 100% buffer B, then a ramp down to 5% buffer B over five min followed by 5% buffer B for 5 min. All peaks were collected, lyophilized, and redissolved in water for characterization via MALDI-MS. For the purification of the caspase-3 (CASP3) CLIP, a similar method was used but the initial gradient was increased from 13% to 27% buffer B over 80 min.

4.5 Synthesis, Purification, and Characterization of FQ-3CL-CLIP

Synthesis of a fluorophore-quencher (FQ) 3CL-CLIP was accomplished using a similar procedure to regular CLIPs as described in **Section 4.4** with a few differences described herein. In place of the Initiator DNA, a Quencher-labeled Initiator DNA containing a 3' black hole quencher (BHQ) was used. In place of Blocking DNA, Dye-labeled Blocking DNA containing a 5' Cy5 dye was used. Care was taken to ensure the materials were stored in dark conditions as well as covered during handling to decrease the chance of them being damaged by ambient light. All conjugation chemistry steps were the same as those used for CLIPs except that the conjugation of linker-peptide-Quencher-labeled Initiator DNA to Dye-labeled Blocking DNA was done over 72 h in a 1:1 ratio. The final product, FQ-3CL-CLIP, was washed using a 3 kDa centrifuge filter 10 times with 0.5 mL of ultrapure water, purified via gel electrophoresis, and characterized via MALDI-MS.

4.6 UV-Vis Characterization

UV-Vis spectroscopy (Agilent, Cary 60 UV-Vis) was used to characterize DNA concentrations, the presence of DNA modifications (e.g., DBCO, dye, quencher, etc.), as well as completion of copper-free click chemistry. A standard 1 cm pathlength cuvette was used.

4.7 MALDI-MS Characterization

MALDI-MS characterization of DNA, peptides, peptide-DNA conjugates, linker-peptide-DNAs, and CLIPs was accomplished using a Bruker AutoFlex Max MALDI-TOF instrument. The matrix utilized for all samples contained 2',6'-dihydroxyacetophenone (DHAP) (Sigma-Aldrich, Cat. No: 37468). The matrix was prepared by dissolving 25 mg of the DHAP in 333 µL of methanol (Fisher Chemical, Methanol (HPLC Grade), Cat. No: A452Sk4) to which 111 µL of saturated ammonium citrate (Sigma-Aldrich, Ammonium Citrate Dibasic, Cat. No: 247561) was added dropwise. A white precipitate was immediately seen and allowed to settle for 15 min. The clear yellow liquid supernatant was used as the matrix. When plating for MALDI-MS, 2 µL of sample was added followed by 1 µL of the DHAP matrix. This resulted in rapid crystallization and was allowed to air dry, ~ 2 min, before MALDI-MS.

To examine the protease cleavage of CLIPs, 1 μM of the 3CL-CLIP was treated with 2 μM 3CL protease (Sigma-Aldrich, Cat. No: SAE0172-200UG) overnight in 3CL Protease Assay Buffer (BPS Bioscience, Cat. No: 79956), with shaking at 1500 rpm at RT. This process took place in a total volume of 100 μL. Subsequently, the solution was washed ten times using a 3 kDa centrifugation filter with 0.5 mL of ultrapure water to remove any salts. The sample remaining in the filter (approximately 10 μL) was then characterized via MALDI-MS.

4.8 PAGE Gel Analysis of CLIPs

4.8.1 Characterization and Purification of CLIPs

Native polyacrylamide gel electrophoresis (PAGE) was utilized to reinforce the MALDI-MS characterization of DNA, peptide-DNA conjugates, linker-peptide-DNAs, and CLIPs. The 15% acrylamide gels, which were produced in-house, were made by diluting a stock 40% acrylamide solution (Bio-Rad, 40% Acrylamide/Bis Solution 19:1, Cat. No: 1610144) with 1X Tris-Borate-EDTA buffer (TBE). The 1X TBE solution was created by diluting 10X TBE (Fisher BioReagents, Tris-Borate-EDTA 10X, Cat. No: BP1333-4) with deionized water.

50 μL N,N,N',N'-Tetramethyl-ethylenediamine (Sigma-Aldrich, N,N,N',N'-Tetramethyl-ethylenediamine, Cat. No: T9281) and ~2 mg of ammonium persulfate (Fisher BioReagents, Ammonium Persulfate (APS) Electrophoresis, Cat. No: BP17) were added to the 15% acrylamide solution to initiate gelation. After mixing well, this solution was poured into a Mini-PROTEAN Tetra Handcast System (Bio-Rad, Cat. No: 1658050). A ten-well comb was placed at the top of the gel, which was allowed to solidify. Following the removal of the comb, the gel wells were thoroughly rinsed with water. The gel was then installed in a Mini-PROTEAN Tetra System (Bio-Rad, Cat. No:1658005EDU) and filled to the manufacturer's recommended line with 1X TBE buffer.

For PAGE characterization, all samples (DNA, peptide-DNA, linker DNA, and CLIPs) were prepared at a final concentration of ~ 1 μM with a total volume of 15 μL. These samples contained 2 μL of glycerol. In addition, a sample containing ultralow DNA molecular weight ladder (Invitrogen, TrackIt Ultra Low Range DNA Ladder, Cat. No: 10488023) was also prepared. The ladder sample was prepared by adding 2 μL of glycerol to 0.2 μL of the ladder stock solution and diluting to a final volume of 15 μL with TBE. 10 μL of all samples were loaded into different wells of the prepared 15% PAGE gel. To track gel progression, 10 μL of a gel loading dye (Sigma-Aldrich, Gel Loading Solution, Cat. No: G7654) was added into a separate dedicated well.

The gel was run at a voltage of 120 V until the loading dye had traveled ~90% of the gel's length, at which point it was stopped. The gel was then removed from the holder, placed in approximately 50 mL of water and stained with GelRed nucleic acid stain (Milipore Sigma, GelRed Nucleic Acid Stain (10,000X, Water), Cat. No: SCT123) for 10 min. Finally, the gel was placed into a Bio-Rad ChemiDoc MP imaging system (Bio-Rad, Cat. No: 12003154), and the GelRed stain was monitored.

Denaturing PAGE was used to purify FQ-3CL-CLIP. As before, a 15% PAGE gel was created. However, the gel also contained 8 M urea (Fisher Chemical, Urea, Cat. No: U15-500). The conditions for running the gel were the same as mentioned above.

For purification, 20 nmol of the FQ-3CL-CLIP was purified via gel electrophoresis. Individual bands could be visualized due to the presence of Cy5 dye and BHQ. These bands were extracted from the gel using a razorblade and placed into 15 mL Falcon tubes. The bands were then crushed using a pipette tip, and 3 mL of deionized water was added to each tube. The mixture was then frozen using liquid nitrogen and thawed three times to aid in the crushing of the gel. Thereafter, the sample was placed on a tube rotator for 48 h. At this point it was noted that the intensity of the color of the gel decreased and that of the surrounding solution increased, indicating that the colored chemical species had migrated into the water. The gel fragments were separated via centrifugation. The supernatant was passed through a fritted syringe, and the filtrate was washed 10 times using a 3 kDa spin filter to remove excess urea. The solution was then characterized via UV-Vis and the presence of purified FQ-3CL-CLIPs were confirmed via MALDI. The approximate yield of this separation was 30%, exceeding what was achieved via HPLC. However, MALDI-MS indicated that this sample was slightly more impure compared to the HPLC-purified CLIPs.

4.8.2 Time-dependent Protease-Mediated Cleavage of CLIPs

Time-dependent cleavage of CLIPs was studied using denaturing PAGE gel. 1 μM FQ-3CL-CLIP was prepared in 3CL buffer with 1 μM 3CL protease. Samples were incubated for 15 min, 30 min, 1 h, 2 h, 4 h, and 6 h. At each point, 2 μL of the solution was mixed with 8 μL of 8 M urea to stop the reaction. A control containing 1 μM FQ-3CL-CLIP without protease was also prepared. Next, 2 μL of glycerol was added to all samples, including the control. Samples were loaded onto a 15% denaturing PAGE gel. To track gel progression, 10 μL of gel loading dye (Sigma-Aldrich, Gel Loading Solution, Cat. No: G7654) was added into a separate well. The gel was run using the same procedure as for native PAGE and monitored in the Cyanine-5 (Cy5) channel.

To study the selectivity of CLIPs, 1 µM FQ-3CL-CLIP was prepared in 3CL and CTSB buffers, spiked with 1 µM 3CL protease and 1 µM CTSB protease, respectively. After incubation for 2 h and 4 h, 2 µL of each solution was mixed with 8 µL of 8 M urea to stop the reaction. A control containing 1 µM FQ-3CL-CLIP without protease was also prepared. Next, 2 µL of glycerol was added to all samples, including the control. Samples were loaded onto a 15% denaturing PAGE gel. To track gel progression, 10 µL of gel loading dye (Sigma-Aldrich, Gel Loading Solution, Cat. No: G7654) was added into a separate well. The gel was run using the same procedure as for native PAGE and monitored in the Cy5 channel.

4.8.3 Stability of CLIPs in Cell Lysates

To study the stability of CLIPs in cell lysates, 1 µM FQ-3CL-CLIP was prepared in PBS and incubated with 5 µL of lysates from the colorectal cancer cell line RKO (CRL-2577) in a total volume of 15 µL. At 30 min, 1 h, 3 h, and 6 h incubation times, 2 µL of the solution was mixed with 8 µL of 8 M urea to stop the reaction. A control containing 1 µM FQ-3CL-CLIP without protease was also prepared. Next, 2 µL of glycerol was added to all samples, including the control. Samples were loaded onto a denaturing PAGE gel prepared as described previously. To track gel progression, 10 µL of gel loading dye (Sigma-Aldrich, Gel Loading Solution, Cat. No: G7654) was added into a separate well. The gel was run using the same procedure as for native PAGE and monitored in the GelRed and Cy5 channels.

4.9 Melting Temperature Analysis

Melting temperature assays were performed to verify the hairpin-like structure of CLIPs. CLIPs containing Dye-labeled Blocking DNA and Quencher-labeled Initiator DNA were used. When CLIPs are folded into a hairpin, close proximity between the fluorophore and the quencher suppresses the fluorescence signal. Dehybridization at higher temperatures opens the hairpin, increases the distance between these molecules, and results in greater fluorescence signal.

All samples were prepared at a concentration of 1 µM in 3CL buffer. To test the effect of protease cleavage on melting temperature, 1 µM of the FQ-3CL-CLIP was incubated with 3 µM of 3CL protease in 3CL buffer overnight for running the melting assay.

Melting assays were conducted by dispensing 10 µL of samples into each well of a 96-well plate (Bio-Rad, Hard-Shell High Profile 96-Well Semi-Skirted PCR Plates, Cat. No: HSS9601), arranging these in triplicate. A qPCR instrument (Bio-Rad, CFX96 Real-Time System C1000 Touch Thermal Cycler) was used for the procedure. The qPCR method was as follows: The lid temperature was consistently maintained at 105°C throughout the assay. Initially, the samples were heated to 90°C over a period of 5 min and then held at this temperature for 30 s. After this, the samples were cooled to 4°C, where the initial fluorescence reading was recorded in the Cy5 channel. The temperature was then increased by 0.5°C increments, with readings taken at each increment in the selected channel. This cycle of increasing temperature and taking readings continued until the temperature reached 95°C.

To account for any photobleaching effects, the fluorescence signal from the Dye-labeled Blocking DNA was used for correction. We also ran additional controls including 3CL buffer, Quencher-labeled Initiator DNA, and 1 µM 3CL protease; as expected, these showed no fluorescence in the Cy5 channel.

4.10 Fluorescence Assays

4.10.1 Optimizing CRISPR-Cas12a Assays

CRISPR-Cas12a ribonucleoprotein (RNP) solution was formed using CRISPR-Cas12a enzyme Alt-R™ L.b. Cas12a (Cpf1) Ultra (Integrated DNA Technologies, Ref. No: 443255472), guide RNA purchased from Integrated DNA Technologies (**Table S2**), and reporter DNase alert (Integrated DNA Technologies, Cat. No: 11-04-03-03). These were prepared in a CRISPR Buffer. To ensure repeatability of CRISPR assays, stock guide RNA and CRISPR-Cas12a were aliquoted into single-use tubes.

All fluorescence experiments were conducted using plate readers. Two types of plate readers were used: Agilent, BioTek Cytation 5 Imaging Multimode Reader and Agilent, BioTek Synergy H1 Multimode Reader. It should be noted that the gain between these plate readers is different and therefore RFU signals may differ between experiments.

We first investigated how the concentration of Initiator DNA affects the fluorescence signal observed in the CRISPR assay. For this, different concentrations of the Initiator DNA (3 nM, 2 nM, 1 nM, 0.5 nM, 0.1 nM, 0 nM) was added to CRISPR buffer containing the RNP (final concentration of 10 nM by Cas12a, 10 nM by gRNA, and 2.5 µL/100 µL total solution of DNase Alert). The fluorescence was measured using a plate reader. Samples were read at 25°C after 30 min using an excitation wavelength of 525 nm and an emission wavelength of 566 nm.

We next investigated how the concentration of the RNP affects the fluorescence signal observed in the CRISPR assay. For this, the Initiator DNA (fixed at a final concentration of 1 nM) was added to CRISPR buffer containing the RNP at various concentrations. The RNP was a 1:1 mixture of Cas12a and the gRNA. The concentrations of RNP used were 100 nM, 10 nM, 1 nM, and 0.1 nM. DNase Alert reporter was added to each well at a concentration of 2.5 µL/100 µL. The fluorescence was measured via plate reader. Samples were read at 25°C and shaken for 30 s before reading fluorescence every three min at an excitation wavelength of 525 nm and an emission wavelength of 566 nm.

4.10.2 Effect of Protease Incubation on the Ability of Initiator DNA to Activate CRISPR-Cas12a Signaling

10 nM Initiator DNA was incubated with and without 3 µM 3CL protease for 2 h with shaking (Benchmark, Multi-Therm Heating Shaker, Cat. No: H5000-H) at 1500 RPM at RT (at 25 °C). Following this, the samples were diluted 10-fold with CRISPR Buffer containing the RNP (final concentration of 10 nM by Cas12a, 10 nM by gRNA, and 2.5 µL/100 µL total solution of DNase Alert). Therefore, the final Initiator DNA concentration while reading fluorescence in the CRISPR assay was 1 nM.

4.10.3 CRISPR-Cas12a Assays with CLIPs

10 nM CLIPs were incubated with varying concentrations of proteases for 30 min-24 h with shaking (Benchmark, Multi-Therm Heating Shaker, Cat. No: H5000-H) at 1500 RPM at RT (at 25 °C). Following this, the samples were diluted 10-fold with CRISPR Buffer containing the RNP (final concentration of 10 nM by Cas12a, 10 nM by gRNA, and 2.5 µL/100 µL total solution of DNase Alert). Therefore, the final CLIP concentration while reading fluorescence in the CRISPR assay was 1 nM.

Here is one example of how solutions were prepared for one assay: Solution 1: 10 nM CLIPs were incubated with proteases in a total of 40 µL of protease-specific assay buffer for 30 min-24 h with shaking at 1500 RPM. Solution 2: A solution of 20 nM CRISPR-Cas12a, 20 nM gRNA, and 5.0 µL/well of DNase alert was prepared in CRISPR-Cas12a assay buffer. When testing protease activity, solution 1 and 2 were added to each well in a black 96 well plate in the following order, 40 µL of CRISPR Buffer, 50 µL of Solution 2, and 10 µL of Solution 1.

4.10.4 Effect of CLIP Concentration on CRISPR-Cas12a Assays

3CL-CLIPs were serially diluted by 10-fold from 10 nM to 10 pM, incubated with 3 µM of 3CL protease for 2 h, and then subjected to the CRISPR-Cas12a assay.

4.10.5 Detection of 3CL, CTSB, MMP7, and CASP3 Proteases in Buffer

10 nM CLIPs targeting various proteases were incubated with their respective proteases for 30 min with shaking (Benchmark, Multi-Therm Heating Shaker, Cat. No: H5000-H) at 1500 RPM at RT (i.e., 25 °C). The proteases used in this study were 3CL (Millipore Sigma, Mpro, 3CL Protease from coronavirus SARS-COV-2, SAE0172), CTSB (Millipore Sigma, Cathepsin B, Human Liver, 219362-50UG), MMP7 (Enzo, MMP-7 catalytic domain, human, recombinant, BML-SE181-0010), and CASP3 (Enzo, Caspase-3 human, recombinant active, ALX-201-059-U025). Protease concentrations used were 500 nM for 3CL, 500 nM for CASP3, 250 nM for MMP7, and 20 nM for CTSB. Each protease was incubated with its corresponding CLIP in its appropriate assay buffer before being subjected to the CRISPR assay. After incubation, the samples were diluted 10-fold with CRISPR Buffer containing the RNP (final concentration of 10 nM by Cas12a, 10 nM by gRNA, and 2.5 µL/100 µL total solution of DNase Alert). Therefore, the final CLIP concentration while reading fluorescence in the CRISPR assay was 1 nM. The fluorescence was measured via plate readers. Samples were read at 25°C and shaken for 30 s before reading fluorescence every 3-5 min at an excitation wavelength of 525 nm and an emission wavelength of 566 nm.

4.10.6 Determination of LOD of 3CL-CLIP

To determine the limit of detection (LOD) for the 3CL-CLIP, 10 nM 3CL-CLIP was incubated with varying concentrations of 3CL protease in 3CL Buffer for 30 min with shaking (Benchmark, Multi-Therm Heating Shaker, Cat. No: H5000-H) at 1500 RPM at RT (at 25 °C). The 3CL protease concentrations used were 500 nM, 250 nM, 125 nM, and 0 nM. Following this, the samples were diluted 10-fold with CRISPR Buffer containing the RNP (final concentration of 10 nM by Cas12a, 10 nM by gRNA, and 2.5 µL/100 µL total solution of DNase Alert). Therefore, the final 3CL-CLIP concentration while reading fluorescence in the CRISPR assay was 1 nM. The fluorescence from the CRISPR assay was read over time using a plate reader (excitation wavelength of 525 nm and an emission at 566 nm). The fluorescence at the 30 min time point from the CRISPR assay was plotted at a function of 3CL concentration to form a calibration curve. From the initial slope of this calibration curve, the LOD was calculated using the 3σ/m method.

4.10.7 Comparison of 3CL-CLIP with DNA only Hairpins

To investigate how CLIP hairpins compare with DNA-only hairpins in their ability to activate CRISPR enzymes, we performed several experiments.

We first investigated how the addition of 24-nt and 16-nt Blocking DNA affects the CRISPR activating capabilities of Initiator DNA. For this, 1 nM of the Initiator DNA was treated with 10 nM of the 16-nt Blocking DNA or 24-nt Blocking DNA. Then CRISPR assays were run (final concentration of 10 nM by Cas12a, 10 nM by gRNA, and 2.5 µL/100 µL total solution of DNase Alert). The fluorescence was measured using a plate reader. Samples were read at 25°C after 30 min using an excitation wavelength of 525 nm and an emission wavelength of 566 nm.

We next conducted CRISPR assays using Initiator DNA, DNA Hairpin 10-8, DNA Hairpin 30-8, and CLIP, each at 1 nM final concentration in the CRISPR assay.

Following this, we investigated how the addition of 24-nt and 16-nt Blocking DNA affects the CRISPR activating capabilities of DNA Hairpin 30-8. For this, 1 nM of the DNA Hairpin 30-8 was treated with 10 nM of the 16-nt Blocking DNA or 24-nt Blocking DNA. Then CRISPR assays were run (final concentration of 10 nM by Cas12a, 10 nM by gRNA, and 2.5 µL/100 µL total solution of DNase Alert). The fluorescence was measured using a plate reader. Samples were read at 25°C after 30 min using an excitation wavelength of 525 nm and an emission wavelength of 566 nm.

4.10.8 Comparison of 3CL-CLIP with 3CL-CFP

To benchmark the protease sensing capabilities of 3CL-CLIP with commercially available probes, a fluorogenic substrate of 3CL (Bio-Techne, SARS CoV-2 3CL protease substrate Rh110-conjugated, Cat. No: S-720-200) was purchased. This probe is referred to as 3CL-CFP.

10 nM 3CL-CLIP was incubated with 250 and 500 nM 3CL protease in 3CL Buffer for 30 min with shaking (Benchmark, Multi-Therm Heating Shaker, Cat. No: H5000-H) at 1500 RPM at RT (at 25 °C). Following this, the samples were diluted 10-fold with CRISPR Buffer containing the RNP (final concentration of 10 nM by Cas12a, 10 nM by gRNA, and 2.5 µL/100 µL total solution of DNase Alert). Therefore, the final 3CL-CLIP concentration while reading fluorescence in the CRISPR assay was 1 nM. The fluorescence from the CRISPR assay was read using a plate reader after an additional 60 min (excitation wavelength of 525 nm and an emission at 566 nm). Therefore, total assay time is 90 min.

For comparison, 10 nM 3CL-CFP was incubated with 250 and 500 nM 3CL protease in 3CL Buffer for 30 min with shaking (Benchmark, Multi-Therm Heating Shaker, Cat. No: H5000-H) at 1500 RPM at RT (at 25 °C). Following this, the samples were diluted 10-fold with CRISPR Buffer. Therefore, the final 3CL-CFP concentration at fluorescence reading was 1 nM. The fluorescence from 3CL-CFP was read using a plate reader after an additional 60 min (excitation wavelength of 485 nm and an emission at 535 nm). Therefore, total assay time is 90 min. This assay was also performed using 1 µM of 3CL-CFP (final probe concentration at fluorescence reading is 100 nM).

4.10.9 Comparison of 3CL-CLIP with FQ-3CL-CLIP

To evaluate the extent of the amplification of the CRISPR-Cas12a system provided on the CLIP signal, a comparison using a FQ-3CL-CLIP was performed.

10 nM 3CL-CLIP was incubated with 250 and 500 nM 3CL protease in 3CL Buffer for 30 min with shaking (Benchmark, Multi-Therm Heating Shaker, Cat. No: H5000-H) at 1500 RPM at RT (at 25 °C). Following this, the samples were diluted 10-fold with CRISPR Buffer containing the RNP (final concentration of 10 nM by Cas12a, 10 nM by gRNA, and 2.5 µL/100 µL total solution of DNase Alert). Therefore, the final 3CL-CLIP concentration while reading fluorescence in the CRISPR assay was 1 nM. The fluorescence from the CRISPR assay was read using a plate reader (excitation wavelength of 525 nm and an emission at 566 nm).

1 µM FQ-3CL-CLIP was incubated with 250 and 500 nM 3CL protease in 3CL Buffer for 30 min with shaking (Benchmark, Multi-Therm Heating Shaker, Cat. No: H5000-H) at 1500 RPM at RT (at 25 °C). Following this, the samples were diluted 10-fold with CRISPR Buffer. Therefore, the final FQ-3CL-CLIP concentration at fluorescence reading was 100 nM. The fluorescence from FQ-3CL-CLIP read using a plate reader (excitation wavelength of 648 nm and an emission at 700 nm). This assay was not performed using 10 nM of FQ-3CL-CLIP (final probe concentration at fluorescence reading is 1 nM) as no fluorescence change could be seen at this concentration.

We performed an additional test with FQ-3CL-CLIP to ensure that the 3CL protease can cleave it. For this, 100 nM FQ-3CL-CLIP was added to 1 µM 3CL protease in 3CL Buffer. The fluorescence from FQ-3CL-CLIP read using a plate reader (excitation wavelength of 648 nm and an emission at 700 nm) over time.

4.10.10 Comparison of CTSB-CLIP with Commercial CTSB Fluorogenic Substrate

To benchmark the protease sensing capabilities of CTSB-CLIP with commercially available probes, a fluorogenic substrate of CTSB (Sigma-Aldrich, Z-Arg-Arg-7-amido-4-methylcoumarin hydrochloride, Cat. No: C5429) was purchased. This probe is referred to as CTSB-CFP.

10 nM CTSB-CLIP was incubated with 10 nM CTSB protease in CTSB Buffer for 30 min with shaking (Benchmark, Multi-Therm Heating Shaker, Cat. No: H5000-H) at 1500 RPM at RT (at 25 °C). Following this, the samples were diluted 10-fold with CRISPR Buffer containing the RNP (final concentration of 10 nM by Cas12a, 10 nM by gRNA, and 2.5 µL/100 µL total solution of DNase Alert). Therefore, the final CTSB-CLIP concentration while reading fluorescence in the CRISPR assay was 1 nM. The fluorescence from the CRISPR assay was read using a plate reader after an additional 120 min (excitation wavelength of 525 nm and an emission at 566 nm). Therefore, total assay time is 150 min.

For comparison, 10 nM CTSB-CFP was incubated with 10 nM CTSB protease in CTSB Buffer for 30 min with shaking (Benchmark, Multi-Therm Heating Shaker, Cat. No: H5000-H) at 1500 RPM at RT (at 25 °C). Following this, the samples were diluted 10-fold with CRISPR Buffer. Therefore, the final CTSB-CFP concentration at fluorescence reading was 1 nM. The fluorescence from CTSB-CFP was read using a plate reader after an additional 120 min (excitation wavelength of 380 nm and an emission at 460 nm). Therefore, total assay time is 150 min.

4.10.11 Determination of LOD of CTSB-CLIP and CTSB-CFP

To determine the limit of detection (LOD) for the CTSB-CLIP, 10 nM CTSB-CLIP was incubated with varying concentrations of CTSB protease in CTSB Buffer for 30 min with shaking (Benchmark, Multi-Therm Heating Shaker, Cat. No: H5000-H) at 1500 RPM at RT (at 25 °C). The CTSB protease concentrations used were 30 nM, 20 nM, 15 nM, 10 nM, 8 nM, 6 nM, 4 nM, 2 nM, 1 nM, and 0 pM. Following this, the samples were diluted 10-fold with CRISPR Buffer containing the RNP (final concentration of 10 nM by Cas12a, 10 nM by gRNA, and 2.5 µL/100 µL total solution of DNase Alert). Therefore, the final CTSB-CLIP concentration while reading fluorescence in the CRISPR assay was 1 nM. The fluorescence from the CRISPR assay was read over time using a plate reader (excitation wavelength of 525 nm and an emission at 566 nm). The fluorescence enhancement at the 120 min time point from the CRISPR assay was plotted at a function of CTSB concentration to form a calibration curve. From the initial slope of this calibration curve, the LOD was calculated using the 3σ/m method.

To determine the limit of detection (LOD) for CTSB-CFP, 1 µM CTSB-CFP was incubated with varying concentrations of CTSB protease (25 nM, 10 nM, 5 nM, 0.1 nM, and 0 nM) in CTSB Buffer for 30 min at 25 °C with shaking at 1500 RPM (Benchmark, Multi-Therm Heating Shaker, Cat. No: H5000-H). After incubation, the samples were diluted 10-fold with CRISPR Buffer, resulting in a final CTSB-CFP concentration of 100 nM during fluorescence measurement. Fluorescence was monitored over time using a plate reader (excitation: 380 nm, emission: 460 nm). Since no fluorescence increase over time was observed, the fluorescence at 0 min was plotted as a function of CTSB concentration to generate a calibration curve. The LOD was calculated from the initial slope of the curve using the 3σ/m method.

4.10.12 Determination of CTSB-CLIP Selectivity

To determine the selectivity of CTSB-CLIP, 10 nM CTSB-CLIP was incubated with 20 nM of different proteases and proteins in CTSB Buffer for 30 min with shaking (Benchmark, Multi-Therm Heating Shaker, Cat. No: H5000-H) at 1500 RPM at RT (at 25 °C). The proteases and proteins used were CTSB, 3CL, MMP7, thrombin (THR), CASP3, and bovine serum albumin (BSA). Following this, the samples were diluted 10-fold with CRISPR Buffer containing the RNP (final concentration of 10 nM by Cas12a, 10 nM by gRNA, and 2.5 µL/100 µL total solution of DNase Alert). Therefore, the final CTSB-CLIP concentration while reading fluorescence in the CRISPR assay was 1 nM. The fluorescence from the CRISPR assay was read after an additional 30 min using a plate reader (excitation wavelength of 525 nm and an emission at 566 nm).

4.10.13 Effect of Nucleases on CLIP Stability

In a low-volume black 384-well plate (Fisher Scientific, Corning™ 384-Well Solid Black or White Polystyrene Microplates, Non-binding, Flat Bottom, Cat. No: 09-761-86), 100 nM FQ-CLIP was prepared in 1X DNase I reaction buffer provided with the DNase I enzyme (Thermo Fisher, DNase I, RNase-free, 1 U/µL, Cat. No: EN0521). To each well, 0.1 U, 0.05 U, 0.025 U, 0.01 U, or 0.001 U of DNase I was added to a total reaction volume of 40 µL. A control containing FQ-3CL-CLIP without DNase I was included. The plate was immediately placed in a plate reader, and fluorescence was measured at an excitation wavelength of 648 nm and an emission wavelength of 700 nm.

4.11 Performance of CLIPs in Serum

10 nM 3CL-CLIP was incubated with 10% human serum (Millipore Sigma, Human Serum, Cat. No: H4522-20ML), with and without 1 µM 3CL protease, for 30 min at 25 °C with shaking at 1500 RPM (Benchmark, Multi-Therm Heating Shaker, Cat. No: H5000-H). After incubation, the samples were diluted 10-fold with CRISPR Buffer containing RNP (final concentrations: 10 nM Cas12a, 10 nM gRNA, and 2.5 µL DNase Alert per 100 µL solution). The final concentrations during fluorescence measurement in the CRISPR assay were 1 nM for 3CL-CLIP and 1% for serum. A control containing 1% serum with RNP was included. For comparison, samples of 3CL-CLIP without serum, with and without 1 µM 3CL protease, were processed concurrently. The fluorescence from the CRISPR assay was read using a plate reader after an additional 15 min (excitation wavelength of 525 nm and an emission at 566 nm).

For comparison, 1 µM 3CL-CFP was incubated with human serum (Millipore Sigma, Human Serum, Cat. No: H4522-20ML), with and without 1 µM 3CL protease, for 30 min at 25 °C with shaking at 1500 RPM (Benchmark, Multi-Therm Heating Shaker, Cat. No: H5000-H). After incubation, samples were diluted 10-fold with CRISPR Buffer, resulting in final concentrations of 100 nM 3CL-CFP and 1% serum during fluorescence measurement in the CRISPR assay. A control containing 1% serum in 90% CRISPR Buffer and 10% 3CL Buffer was also prepared. For comparison, samples of 3CL-CFP without serum, with and without 1 µM 3CL protease, were processed concurrently. The fluorescence from 3CL-CFP was read using a plate reader after an additional 15 min (excitation wavelength of 485 nm and an emission at 535 nm).

4.12 Cell Culture and Sample Preparation

The primary cell lines used in this study were NCI-H508 (CCL-253), RKO (CRL-2577), HT29 (HTB-38), and SW-620 (CCL-227). Every primary cell line was purchased from the American Type Culture Collection (ATCC) and cultivated in RPMI-1640, fortified with 10% fetal bovine serum, 1% penicillin/streptomycin, 1% Glutamax, 1% non-essential amino acids (sourced from Gibco), and 10 mM HEPES, and kept in an environment-controlled incubator at 37ºC with 5% CO_2.

2,000,000 viable cells were seeded into 6 cm tissue culture plates and left to incubate overnight. For intracellular protease analysis, the cells were first rinsed with PBS (provided by Gibco) to remove extracellular proteases, then physically dislodged via cell scraping into 1 mL PBS. This solution was then lysed via sonication. The sample was alternately placed in a bath sonicator for 5 s and on ice for 5 s for a total of 5 times. The cells were next collected into a pellet by centrifuging the solution at 16.2x g at a temperature of 4ºC for a duration of 15 min. The supernatant was collected for analysis.

4.13 Detection of Active Proteases in Cell Lysates

4.13.1 Detection of 3CL Protease in 3CL-Spiked Cell Lysates Using 3CL-CLIPs

To determine the ability of CLIPs to detect a specific protease of interest in complex media, NCI-H508 lysates were spiked with 3CL protease and treated with 3CL-CLIPs. The presence of SARS CoV-2 proteases in these samples is not expected. Therefore, the fluorescence from 3CL-CLIP in the absence of the 3CL protease serves as an estimate of the background in these systems.

10 nM of 3CL-CLIP was incubated with 15 µL of the cell lysates (~2 million cells/mL) in a total volume of 45 µL of 3CL Buffer with or without 1 µM 3CL protease. The samples were then incubated for 30 min with shaking (Benchmark, Multi-Therm Heating Shaker, Cat. No: H5000-H) at 1500 RPM at RT (at 25 °C). Following this, the samples were diluted 10-fold with CRISPR Buffer containing the RNP (final concentration of 10 nM by Cas12a, 10 nM by gRNA, and 2.5 µL/100 µL total solution of DNase Alert). Therefore, the final 3CL-CLIP concentration while reading fluorescence in the CRISPR assay was 1 nM. The fluorescence from the CRISPR assay was read using a plate reader after an additional 30 min (excitation wavelength of 525 nm and an emission at 566 nm). Therefore, total assay time is 60 min.

4.13.2 Detection of CTSB Protease in Cell Lysates Using CTSB-CLIP

To detect active proteases in complex media, lysates derived from different colon cancer cell lines (NCI-H508, SW-620, RKO, and HT29) were treated with CLIPs. In these cell samples, CTSB is expected to have high activity levels based on previous studies.[60,67,73,74] Therefore, fluorescence from CTSB-CLIP will be correlated to the activity of CTSB protease. On the other hand, the presence of SARS CoV-2 proteases in these samples is not expected. Therefore, the fluorescence from 3CL-CLIP will serve as an estimate of the background in these systems.

10 nM of CLIPs were incubated with 15 µL of the cell lysates (~2 million cells/mL) in a total volume of 45 µL of 1X PBS. The samples were then incubated for 30 min with shaking (Benchmark, Multi-Therm Heating Shaker, Cat. No: H5000-H) at 1500 RPM at RT (at 25 °C). Following this, the samples were diluted 10-fold with CRISPR Buffer containing the RNP (final concentration of 10 nM by Cas12a, 10 nM by gRNA, and 2.5 µL/100 µL total solution of DNase Alert). Therefore, the final CTSB-CLIP concentration while reading fluorescence in the CRISPR assay was 1 nM. The fluorescence from the CRISPR assay was read using a plate reader after an additional 30 min (excitation wavelength of 525 nm and an emission at 566 nm). Therefore, total assay time is 60 min.

Additional experiments were performed using 5 µL, 3 µL, and lower volumes of the cell lysates. However, no signal was observed for samples containing <3 µL lysates.

4.13.3 Detection of CTSB Protease in Cell Lysates with Commercial CTSB Reporter

1 µM of CTSB-CFP was incubated with 15 µL of various cell lysates (~2 million cells/mL) in a total volume of 45 µL of 1X PBS. The samples were then incubated for 30 min with shaking (Benchmark, Multi-Therm Heating Shaker, Cat. No: H5000-H) at 1500 RPM at RT (at 25 °C). Following this, the samples were diluted 10-fold with CRISPR Buffer. Therefore, the final CTSB-CFP concentration at fluorescence reading was 100 nM. The fluorescence from CTSB-CFP was read using a plate reader after an additional 30 min (excitation wavelength of 380 nm and an emission at 460 nm). Therefore, total assay time is 60 min.

4.13.4 Effect of CTSB Inhibitor on Fluorescence Signal from CTSB-CLIP and CTSB-CFP

To further confirm that the fluorescence signal observed from CTSB-CLIP and CTSB-CFP in the presence of cell lysates stems from the activity of CTSB protease, we performed additional experiments with a well-known CTSB inhibitor (Sigma-Aldrich Cathepsin Inhibitor II, Cat. No: 219385-1MG). We reasoned that the presence of this inhibitor would lead to a reduction in the fluorescence signal, thereby confirming its dependency on CTSB protease activity.

10 nM of CTSB-CLIP was incubated with 6 µL of RKO cell lysates (~2 million cells/mL) in a total volume of 45 µL of 1X PBS with or without 667 µM CTSB inhibitor. The samples were then incubated for 30 min with shaking (Benchmark, Multi-Therm Heating Shaker, Cat. No: H5000-H) at 1500 RPM at RT (at 25 °C). Following this, the samples were diluted 10-fold with CRISPR Buffer containing the RNP (final concentration of 10 nM by Cas12a, 10 nM by gRNA, and 2.5 µL/100 µL total solution of DNase Alert). Therefore, the final CTSB-CLIP concentration while reading fluorescence in the CRISPR assay was 1 nM. The fluorescence from the CRISPR assay was read using a plate reader after an additional 60 min (excitation wavelength of 525 nm and an emission at 566 nm). Therefore, total assay time is 90 min.

1 µM of CTSB-CFP was incubated with 6 µL of RKO cell lysates (~2 million cells/mL) in a total volume of 45 µL of 1X PBS with or without 667 µM CTSB inhibitor. The samples were then incubated for 30 min with shaking (Benchmark, Multi-Therm Heating Shaker, Cat. No: H5000-H) at 1500 RPM at RT (at 25 °C). Following this, the samples were diluted 10-fold with CRISPR Buffer. Therefore, the final CTSB-CFP concentration while reading fluorescence in the CRISPR assay was 100 nM. The fluorescence from CTSB-CFP was read using a plate reader after an additional 60 min (excitation wavelength of 380 nm and an emission at 460 nm). Therefore, total assay time is 90 min.

5 Data Analysis

All data reported is the average of at least 3 replicate measurements unless otherwise mentioned. Error bars represent the standard deviation of these measurements.

Normalized fluorescence is calculated by normalizing the highest fluorescence value in a data set to 100%. Normalized fluorescence is used for **Figures 2** and **3**.

Fluorescence enhancement is defined as the ratio of the fluorescence values of a sample (I_f) to the fluorescence of the RNP complex (I_{RNP}) or buffer (I_{buffer}) at a given timepoint. During error propagation, error from the denominator is ignored. Fluorescence enhancement was calculated using **Equation 1:**

$$Fluorescence\ Enhancement = \frac{I_f}{I_{RNP}\ or\ I_{buffer}} \qquad eq\ (1)$$

Relative fluorescence is defined as the ratio of the fluorescence values of a sample treated with protease ($I_{+Protease}$) to the fluorescence values the sample without protease ($I_{-Protease}$) at the same time point. During error propagation, error from the denominator is ignored. Relative fluorescence was calculated using **Equation 2:**

$$Relative\ Fluorescence = \frac{I_{+Protease}}{I_{-Protease}} \qquad eq\ (2)$$

Corrected normalized fluorescence is used in melting temperature analysis shown in **Figure 2B**. In this experiment, fluorescence of FQ-3CL-CLIP is expected to increase with rising temperature due to enhanced separation between the fluorophore and the quencher. However, since fluorescence itself can vary with temperature, we conducted control experiments using only Dye-labeled Blocking DNA to adjust for this temperature dependence. The fluorescence readings from the Dye-labeled Blocking DNA at various temperatures ($I_{Dye-labeled\ Blocking\ DNA,T}$) were used to correct for the fluorescence values in other samples ($I_{sample,\ T}$). The temperature-corrected fluorescence value ($I_{corrected,T}$) is given by **Equation 3**:

$$I_{corrected,T} = \frac{I_{Dye-labeled\ Blocking\ DNA,4°C}}{I_{Dye-labeled\ Blocking\ DNA,T}} * I_{sample,T} \qquad eq\ (3)$$

Subsequently, the maximum fluorescence value observed across the data set was assigned a value of 100, while the minimum was set to 0 to correct for background noise. All other fluorescence readings were scaled between these two extremes accordingly. Corrected normalized fluorescence was calculated using **Equation 4:**

$$Corrected\ Normalized\ Fluorescence = \frac{I_{corrected,T} - I_{corrected,4°C}}{I^{max}_{corrected,T} - I_{corrected,4°C}} * 100 \qquad eq\ (4)$$

Relative abundance (%) is used for showing mass spectrometry data in **Figure 2A**. It is calculated by setting the highest m/z value to 100%.

6 Additional Results and Discussion

6.1 T_m Analysis

To determine what proportion of the initiator strand must be hybridized to the blocking strand so that the CLIP remains in a hairpin-like structure at room temperature (25 °C), we performed T_m analysis using IDT OligoAnalyzer™ on hairpins comprised entirely of DNA. To closely mimic the structure of CLIPs, the non-DNA portion of the CLIP was replaced with DNA of comparable length. The contour length of amino acids ranges from 0.36 nm to 0.4 nm, the PEG linker's length is approximately 1.4 nm,[75] and the length of ssDNA is reported to be between 0.3 nm to 0.6 nm per base.[76-78] Therefore, the non-DNA portion of the CLIP (which can be between 6.4-6.8 nm in length if the CLIP has 10 aa) can be approximated using ssDNA containing 10-30 bases.

We modeled the T_m of DNA hairpins of the form $I_{24}X_{10}B_n$ and $I_{24}X_{30}B_n$. I_{24} represents the initiator strand containing 24 bases. X represents ssDNA bases used to mimic the non-DNA portion of the CLIP. B_n represents the blocking strand containing n bases ($n = 2 - 13$). Hairpins of the form $I_{24}X_{10}B_n$ have a stem length of n base pairs and a loop size of $24 - n + 10$. Hairpins of the form $I_{24}X_{30}B_n$ have a stem length of n base pairs and a loop size of $24 - n + 30$. The loop size decreases as the number of bases in the blocking strand increases.

After proteolytic cleavage, CLIPs are expected to form an intermolecular duplex with lower T_m compared to the hairpin-like structure. To estimate the T_m of the DNA duplex formed after proteolysis, we also computed the T_m of dsDNA with n bases. The sequence of these bases is identical to the sequence in the stem portion of the hairpins. All calculated T_m are shown in degree Celsius in **Table S3**-**Table S6**.

The results indicate that CLIPs with 5-9 base pairs in the stem would maintain hairpin-like structures under the different assay conditions used (DNA concentration 1-10 nM; 100-300 mM Na^+; 20-40 mM Mg^{2+}) but would dissociate upon proteolytic cleavage. We chose 8 base pairs as the optimal stem length. This range encompasses what is typically understood as physiological ionic strength (~150 mM).

Structures of DNA hairpins of the form $I_{24}X_{30}B_8$ and $I_{24}X_{10}B_8$ are shown in **Figure S4**.

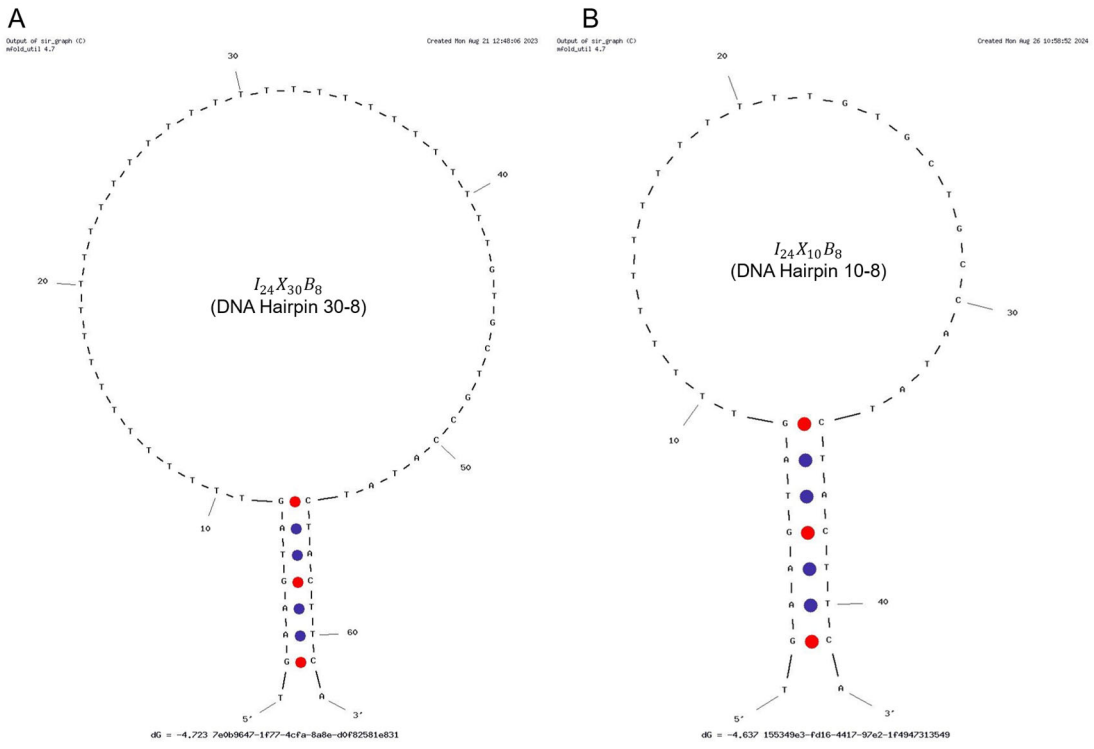

Figure S4. Structures of DNA hairpins of the form (A) $I_{24}X_{30}B_8$ (DNA Hairpin 30-8) and (B) $I_{24}X_{10}B_8$ (DNA Hairpin 10-8).

Table S3. T_m analysis of DNA structures. The top section presents the T_m of DNA hairpins of the form $I_{24}X_{10}B_n$. The lower section shows the T_m for dsDNA corresponding to the stem lengths of the hairpins.

T_m values are expressed in degrees Celsius. Calculations were performed using IDT Oligo Analyzer™ under conditions of 40 mM Mg^{2+} and 100 mM Na^{+}. The hairpin/dsDNA concentrations tested were 0.1 nM, 1 nM, and 10 nM. NH indicates that a desirable hairpin structure is not formed.

	Number of Base Pairs in Hairpin Stem											
Hairpin Concentration (nM)	2	3	4	5	6	7	8	9	10	11	12	13
0.1	NH	NH	15	35.3	41.1	44.4	53.2	57.4	58.5	60.9	61.8	65.9
1	NH	NH	15	35.3	41.1	44.4	53.2	57.4	58.5	60.9	61.8	65.9
10	NH	NH	15	35.3	41.1	44.4	53.2	57.4	58.5	60.9	61.8	65.9

	Number of Base Pairs in Cleaved Hairpin dsDNA											
dsDNA Concentration (nM)	2	3	4	5	6	7	8	9	10	11	12	13
0.1	0	0	0	0	0	0	0	7.2	13.1	17	21.3	27
1	0	0	0	0	0	0	5.6	13.4	18.8	22.3	26.3	31.5
10	0	0	0	0	0	0.8	12.4	19.8	24.8	27.8	31.4	36.2

Table S4. T_m analysis of DNA structures. The top section presents the T_m of DNA hairpins of the form $I_{24}X_{10}B_n$. The lower section shows the T_m for dsDNA corresponding to the stem lengths of the hairpins.

T_m values are expressed in degrees Celsius. Calculations were performed using IDT Oligo Analyzer™ under conditions of 40 mM Mg^{2+} and varying Na^+. DNA concentration was kept at 1 nM. NH indicates that a desirable hairpin structure is not formed.

Na^+ Concentration (mM)	Number of Base Pairs in Hairpin Stem											
	2	3	4	5	6	7	8	9	10	11	12	13
10	NH	NH	14.6	34.8	40.6	43.9	52.7	56.8	57.9	60.2	61.1	65.2
100	NH	NH	15	35.3	41.1	44.4	53.2	57.4	58.5	60.9	61.8	65.9
300	NH	NH	15.8	36.1	42	45.4	54.2	58.5	59.6	62	63	67.1

Na^+ Concentration (mM)	Number of Base Pairs in Cleaved Hairpin dsDNA											
	2	3	4	5	6	7	8	9	10	11	12	13
10	0	0	0	0	0	0	5.6	13.4	18.9	22.5	26.4	28.8
100	0	0	0	0	0	0	5.6	13.4	18.8	22.3	26.3	31.5
300	0	0	0	0	0	0	6.8	14.5	19.9	23.3	27.2	32.4

Table S5. T_m analysis of DNA structures. The top section presents the T_m of DNA hairpins of the form $I_{24}X_{10}B_n$. The lower section shows the T_m for dsDNA corresponding to the stem lengths of the hairpins.

T_m values are expressed in degrees Celsius. Calculations were performed using IDT Oligo Analyzer™ under conditions of varying Mg^{2+} concentrations and 100 mM Na^+. DNA concentration was kept at 1 nM. NH indicates that a desirable hairpin structure is not formed.

Mg^{2+} Concentration (mM)	Number of Base Pairs in Hairpin Stem											
	2	3	4	5	6	7	8	9	10	11	12	13
0	NH	NH	8.9	28.1	33.2	36.2	44.8	48.2	49	51.2	51.8	55.8
20	NH	NH	14.1	34.2	39.9	43.2	52	56	57.1	59.4	60.3	64.4
40	NH	NH	15	35.3	41.1	44.4	53.2	57.4	58.5	60.9	61.8	65.9

Mg^{2+} Concentration (mM)	Number of Bases in Cleaved Hairpin dsDNA											
	2	3	4	5	6	7	8	9	10	11	12	13
0	0	0	0	0	0	0	0	4.2	9.8	13.5	17.5	23.4
20	0	0	0	0	0	0	5.1	12.9	18.3	21.8	25.8	31.1
40	0	0	0	0	0	0	5.6	13.4	18.8	22.3	26.3	31.5

Table S6. T_m analysis of DNA hairpins of the form $I_{24}X_{10}B_n$ and $I_{24}X_{30}B_n$. The top section presents the T_m of DNA hairpins at 20 mM Mg^{2+} concentrations. The lower section shows the T_m of DNA hairpins at 40 mM Mg^{2+} concentrations.

T_m values are expressed in degrees Celsius. Calculations were performed using IDT Oligo Analyzer™ at 100 mM Na^+. DNA concentration was kept at 1 nM. NH indicates that a desirable hairpin structure is not formed.

	Number of Base Pairs in Hairpin Stem											
	2	3	4	5	6	7	8	9	10	11	12	13
X_{10}	NH	NH	14.1	34.2	39.9	43.2	52	56	57.1	59.4	60.3	64.4
X_{30}	NH	NH	NH	29.4	35.1	38.5	47.5	51.4	52.4	54.4	55.3	59.5

	Number of Base Pairs in Hairpin Stem											
	2	3	4	5	6	7	8	9	10	11	12	13
X_{10}	NH	NH	15	35.3	41.1	44.4	53.2	57.4	58.5	60.9	61.8	65.9
X_{30}	NH	NH	NH	30.4	36.2	39.7	48.7	52.7	53.8	55.8	56.7	60.9

6.2 MALDI-MS Data

6.2.1 MALDI-MS Data of 3CL, CASP3, CTSB, and MMP7-CLIPs and Intermediates

Table S7. Expected (Ex) Versus Observed (Ob) MALDI *m/z* of CLIPs and Intermediate Species

CLIP	3CL (m/z)		CTSB (*m/z*)		CASP3 (m/z)		MMP7 (m/z)	
	Ex	Ob	Ex	Ob	Ex	Ob	Ex	Ob
Peptide-DNA Conjugate	8,895	9,028	8,862	8,895	8,879	8,992	9,200	9,140
Peptide-DNA Linker	9,331	9,292	9,152	9,226	9,169	9,299	9,490	9,711
CLIP	12,569	12,608	12,702	12,491	12,715	12,932	13,040	13,003
Pure CLIP	12,569	12,608	12,702	12,460	12,715	12,782	13,040	12,995

6.2.2 MALDI-MS Data of Fluorophore Quencher CLIP

Table S8. Expected Versus Observed MALDI m/z of FQ-3CL-CLIP

Name	Expected Molecular Weight (Da)	Observed Molecular Weight *(m/z)*	Quencher Extinction Absorbance Range	Fluorophore Absorbance Max
FQ-3CL-CLIP	13,502	13,325	560-670 nm	649 nm

6.3 UV-Vis Characterization of CLIPs

First, peptide-DNA conjugates were synthesized through copper free click chemistry using azido-peptides and dibenzocyclooctyne (DBCO) modified DNA. Initiator DNA was treated with increasing concentrations of azide pep-3CL for 24 h and the reaction progression was observed through monitoring the DBCO's characteristic 310 nm absorbance. Treatment of 0:1, 1:1, 3:1, and 5:1, azide to DBCO was measured. In samples of 3:1 and 5:1 equivalents the 310 nm peak appears to have disappeared fully indicating a complete conjugation (**Figure S5**). Therefore, all DBCO azide click chemistry used at least a 3:1 ratio to ensure complete product conversion unless otherwise noted.

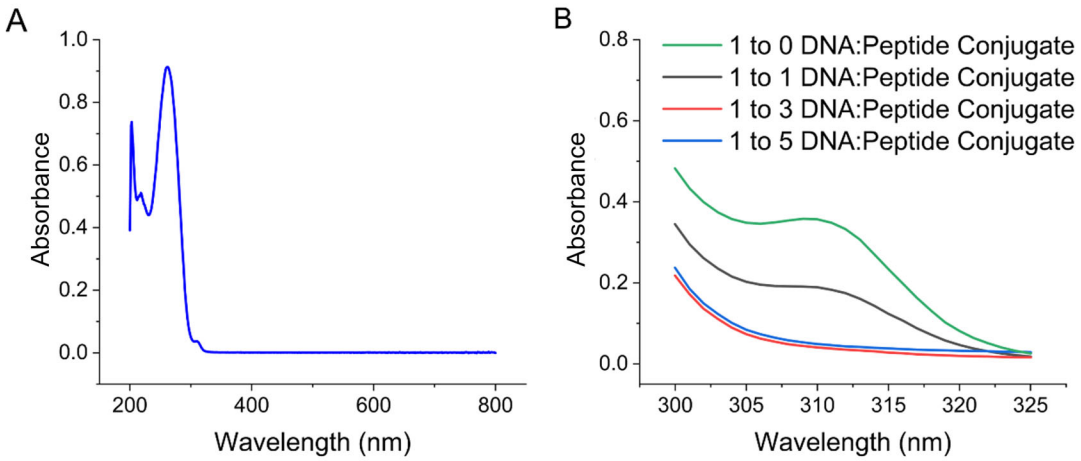

Figure S5. (A) The UV-Vis spectra of Initiator DNA. DNA's characteristic peak at 260 nm as well as the DBCO's characteristic 310 nm peak. (B) Initiator DNA treated with increasing concentrations of azide pep-3CL after 24 h. From the conjugation of DBCO to azide groups, the 310 nm peak decreases indicating successful conjugation of peptide-DNA conjugates. Treatment of 0:1, 1:1, 3:1, and 5:1, azide to DBCO was measured. In samples of 3:1 and 5:1 equivalents the 310 nm peak appears to have disappeared indicating a successful complete conjugation.

Next, an azido PEG linker was installed on the peptide-DNA conjugate. The final CLIP structure (i.e. the DNA-peptide-DNA triblock) was synthesized by reacting linker-peptide-DNAs with Blocking DNA using copper free click chemistry. UV-Vis spectroscopy was used to confirm attachment of Blocking DNA to peptide-DNA linkers. 5:1 molar ratio was used with respect to DBCO Blocking DNA to peptide-DNA linkers. Therefore, with 100% conjugation a 20% absorbance decrease at 310 nm is theoretically expected. Upon treatment the DBCO's characteristic absorbance at 310 nm decreases approx. 18%, indicating that the azide on the peptide-DNA linker has successfully conjugated (**Figure S6**).

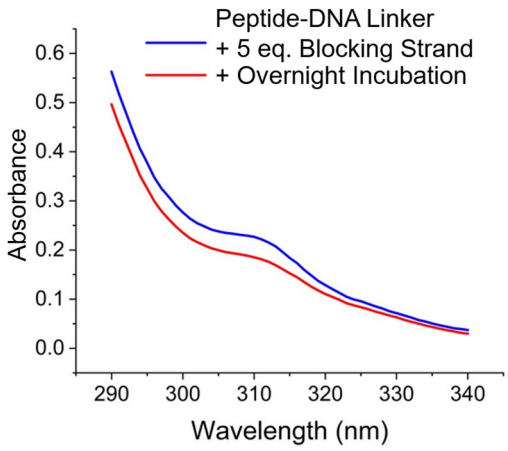

Figure S6. UV-Vis spectra of peptide-DNA linker before (blue) and after (red) overnight incubation with blocking strand DNA. Upon treatment the DBCO's characteristic absorbance at 310 nm decreases approx. 18%, indicating that the azide on the peptide-DNA linker has successfully been attached.

6.4 Gel Electrophoresis Characterization of CLIPs

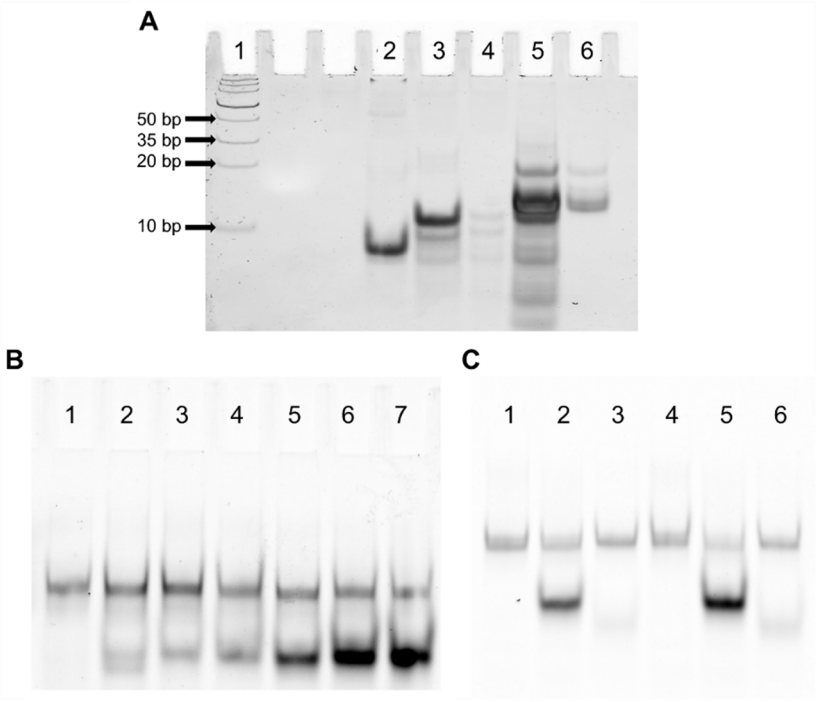

Figure S7. (A) Native PAGE gel containing (1) Invitrogen™ Trackit™ Ultra Low Range DNA Ladder, (2) Initiator DNA, (3) 3CL peptide-DNA conjugates, (4) 3CL peptide-DNA-linker conjugates, (5) impure CLIPs, and (6) HPLC-purified CLIPs. All samples are loaded in approximately 10 pmol amounts. The mobility of the structures gradually decreases with the addition of each component, indicating successful conjugation. Between impure and purified CLIPs species correlating to Initiator DNA, peptide-DNA conjugates, and peptide-DNA-linker conjugates, are all seen to disappear. Also note that multiple bands also appear on this gel for CLIPs possibly due to differences in either conformation or hybridization of the species. Lane 4 corresponds to the DNA-Peptide-Linker species which appears lighter than other species even at the same concentration. The reason for this effect is unknown but has been previously observed in these molecules by others.[52] We speculate that the addition of both the peptide and PEG linker affects the staining of the DNA.

(B) Denaturing PAGE gel showing time-dependent 3CL-mediated cleavage of FQ-3CL-CLIP. Lane 1 shows the intact FQ-3CL-CLIP, while lanes 2–7 represent samples incubated with 1 μM 3CL protease for varying durations: 15 min, 30 min, 1 h, 2 h, 4 h, and 6 h, respectively. Approximately 2 pmol of each sample was loaded onto the gel, which was imaged using the Cy5 fluorescence channel. Following protease treatment, a new band with higher mobility appears, corresponding to the cleaved fragment. Over time, the intensity of the original FQ-3CL-CLIP band diminishes, while the intensity of the cleaved fragment band increases, indicating progressive and successful proteolytic cleavage of FQ-3CL-CLIP. It should be noted that the intact CLIP structure contains both Cy5 and its quencher, BHQ. As the CLIP degrades, Cy5 and BHQ separate, causing an increase in Cy5 fluorescence relative to the intact structure. This artificially enhances the intensity of the fragment bands in the Cy5 channel, making the proportion of fragments appear higher than it actually is.

(C) Denaturing PAGE gel showing selectivity of FQ-3CL-CLIP. Lanes 1 and 4 show untreated FQ-3CL-CLIP samples after 2 h and 4 h, respectively. Lanes 2 and 5 represent FQ-3CL-CLIP incubated with 1 μM 3CL protease for 2 h and 4 h, respectively. Lanes 3 and 6 correspond to FQ-3CL-CLIP incubated with 1 μM CTSB protease for 2 h and 4 h, respectively. Approximately 2 pmol of each sample was loaded onto the gel. After incubation with 3CL protease, a new band with higher mobility appears, indicating successful cleavage of FQ-3CL-CLIP. Over time, the intensity of the original FQ-3CL-CLIP band diminishes, while the intensity of the cleaved fragment band increases, indicating progressive and successful proteolytic cleavage of FQ-3CL-CLIP. In contrast, incubation with CTSB protease also generates a new band, but with much lower intensity relative to the 3CL protease-treated samples. This observation highlights the preference of 3CL protease for FQ-3CL-CLIP over CTSB protease, demonstrating the higher selectivity of 3CL protease for this substrate. It should be noted that the intact CLIP structure contains both Cy5 and its quencher, BHQ. As the CLIP degrades, Cy5 and BHQ separate, causing an increase in Cy5 fluorescence relative to the intact structure. This artificially enhances the intensity of the fragment bands in the Cy5 channel, making the proportion of fragments appear higher than it actually is.

6.5 CRISPR-Cas12a Assays with 3CL-CLIP

6.5.1 Optimizing CRISPR-Cas12a Assays

We first determined the optimal conditions for CRISPR-Cas12a assays. Specifically, we investigated how the concentration of Initiator DNA (**Figure S8**) and the RNP complex (**Figure S9**) affect the fluorescence signal observed.

Next, we verified that incubating the Initiator DNA alone with proteases does not impact the CRISPR signal (**Figure S10**). Following this, we performed CRISPR assays with 3CL-CLIPs in the presence and absence of proteases. It is important to note that 3CL-CLIPs must be purified from any free Initiator DNA or else background signal is observed (**Figure S11**). Moreover, the fluorescence signal is affected by the concentration of 3CL-CLIP used in the CRISPR assay (**Figure S12**).

Based on our results, we identified that 1 nM 3CL-CLIP and 10 nM RNP are optimal for our assays. Under these conditions, the limit of detection of 3CL-CLIP is 116 nM (**Figure S13**).

6.5.2 Effect of Initiator DNA Concentration on CRISPR-Cas12a Assays

To evaluate which concentration of DNA is most optimal for CRISPR-Cas12a assays, RNP was held at a constant 10 nM was treated with increasing concentrations of Initiator DNA. It was observed that an increased concentration of Initiator DNA correlates to an increased CRISPR-Cas12a fluorescent response. Concentrations above 1 nM show larger standard deviation in triplicate and odd trends while concentrations at or below 0.1 nM show minimal signal. To balance both a need for high signal, high repeatability, and to use fewer reagents a concentration of 1 nM Initiator DNA was chosen as optimal.

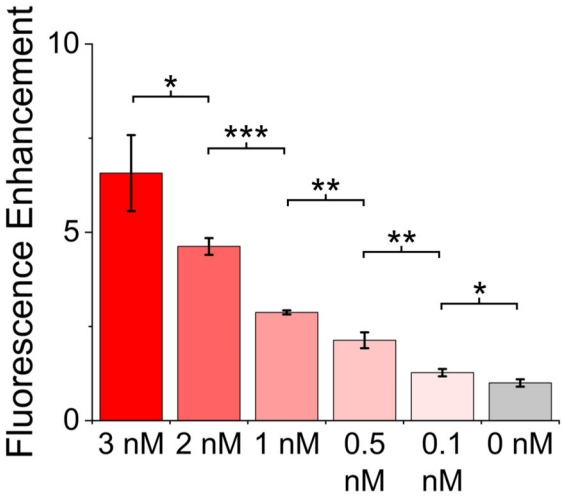

Figure S8. Fluorescence enhancement observed from treatment of 10 nM RNP with varied concentrations of the Initiator DNA after 30 min. Fluorescence enhancement refers to the fluorescence of a sample relative to the fluorescence of the RNP. *, **, and *** denote statistical significance at the 95%, 99%, and 99.9% confidence levels, respectively, assessed using a one-tailed Student's t-test.

6.5.3 Effect of Increasing RNP Concentration on CRISPR-Cas12a Assays

To discover an optimal RNP concentration for CRISPR assays, a fixed concentration of Initiator DNA (1 nM) was treated with RNP at concentrations of 100 nM, 10 nM, 1 nM and 0.1 nM. These samples were then subjected to CRISPR assays. Concentrations of RNP below 1 nM show incomplete saturation within 60 min while concentrations around 10 nM saturate within the time frame. An RNP concentration of 10 nM was chosen due to its ability to saturate within 1 h with 1 nM of Initiator DNA.

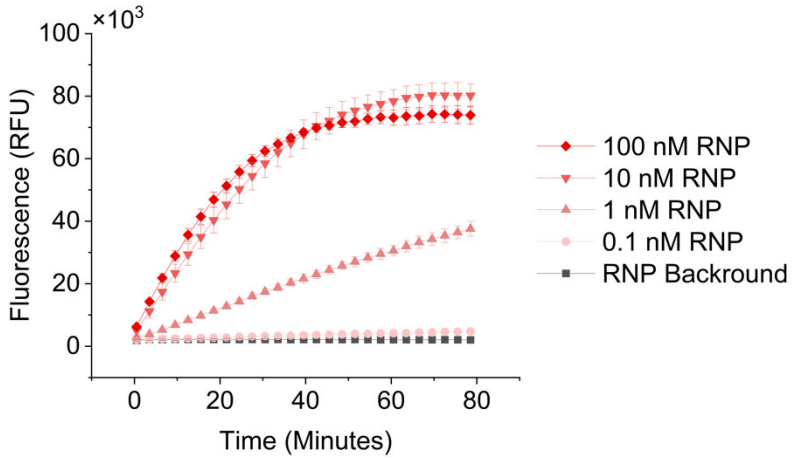

Figure S9. Time-dependent fluorescence assay showing signal response from treating 1 nM Initiator DNA with varied concentration of RNP.

6.5.4 Effect of Protease Incubation on the Ability of Initiator DNA to Activate CRISPR-Cas12a Signaling

To investigate whether incubation of the Initiator DNA with proteases affect CRISPR assays, 10 nM of Initiator DNA was incubated with 3 μM 3CL protease for 2 h and then subjected to a CRISPR assay. In doing so there was no change seen with the activation of the Initiator DNA with and without protease incubation. This implies that 3CL protease does not interfere with the binding and activation of Initiator DNA with RNP complexes.

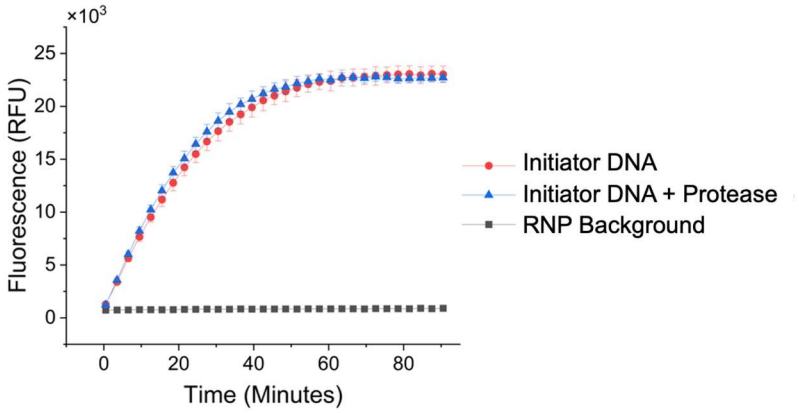

Figure S10. Time-dependent CRISPR-Cas12a detection of Initiator DNA before and after treatment with 3 μM 3CL protease.

6.5.5 Effect of Purification of 3CL-CLIP on CRISPR-Cas12a Response

Impure and HPLC purified samples at 10 nM 3CL-CLIPs were incubated with 3 μM 3CL protease for 2 h and diluted 10-fold with CRISPR buffer before running a CRISPR assay. The final probe concentration in the CRISPR assay was 1 nM. Impure CLIPs show high background, likely due to the presence of non-hairpinning unreacted species, while after HPLC purification, CLIP mixtures show retention of the same signal seen in impure samples but with the decrease of signal in unincubated samples.

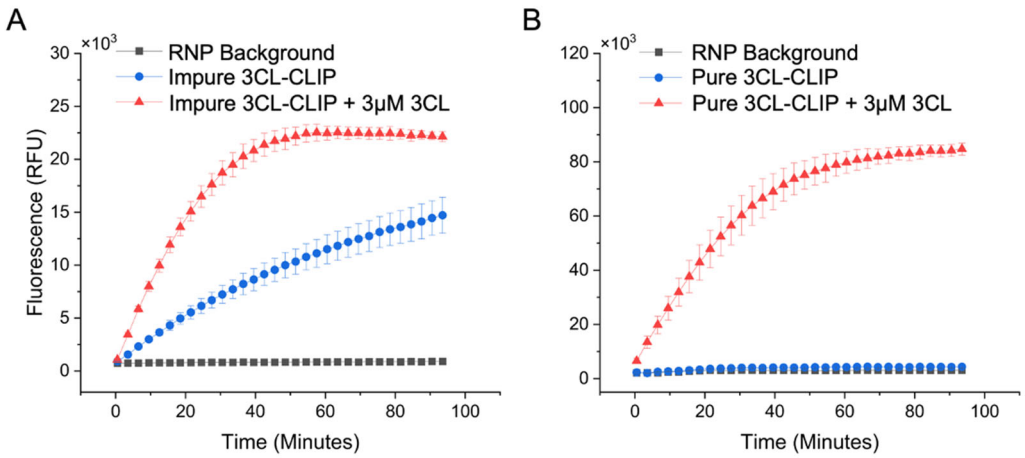

Figure S11. Time-dependent CRISPR-Cas12a fluorescence assays upon incubating 1 nM of (A) impure and (B) purified 3CL-CLIPs with 3CL protease.

6.5.6 Effect of CLIP Concentration on CRISPR-Cas12a Assays

3CL-CLIPs were serially diluted by 10-fold from 10 nM to 10 pM, incubated with 3 μM of 3CL protease for 2 h, and then subjected to the CRISPR-Cas12a fluorescence assay. Minimal increase in fluorescence is observed using CLIP concentrations below 0.1 nM, whereas 10 nM CLIPs begin to show background signal in the absence of protease. Therefore, an optimal concentration of 1 nM CLIPs (in the final CRISPR buffer) was used for subsequent experiments.

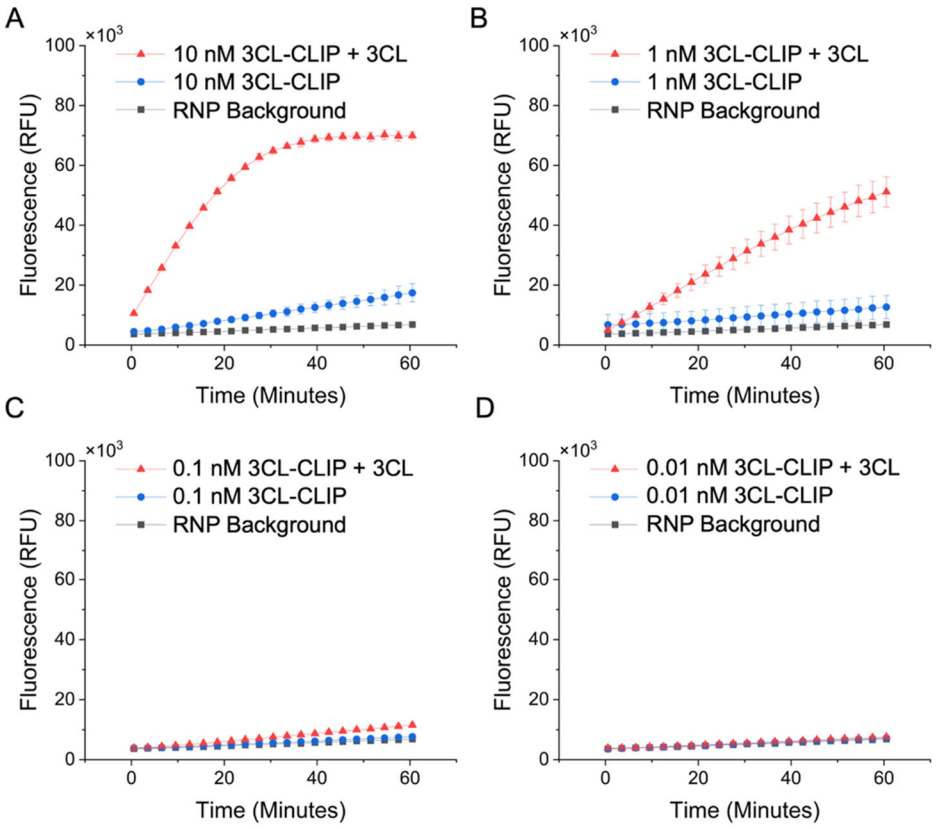

Figure S12. Signal increase upon incubating (A) 10 nM, (B) 1 nM, (C) 0.1 nM, and (D) 10 pM, of 3CL-CLIPs with 3CL protease.

6.5.7 Limit of Detection of 3CL-CLIPs

To determine the limit of detection (LOD) for the 3CL-CLIP, 10 nM 3CL-CLIP was incubated with varying concentrations of 3CL protease (500 nM, 250 nM, 125 nM, and 0 nM) in 3CL Buffer for 30 min with at RT (at 25 °C). Following this, the samples were diluted 10-fold with CRISPR Buffer containing the RNP (final concentration of 10 nM by Cas12a, 10 nM by gRNA, and 2.5 µL/100 µL total solution of DNase Alert). Therefore, the final 3CL-CLIP concentration while reading fluorescence in the CRISPR assay was 1 nM. The fluorescence from the CRISPR assay was read over time. The fluorescence at the 30 min time point from the CRISPR assay was plotted as a function of 3CL concentration to form a calibration curve. From the initial slope of this calibration curve, the LOD was calculated using the 3σ/m method. The LOD was found to be 116 nM.

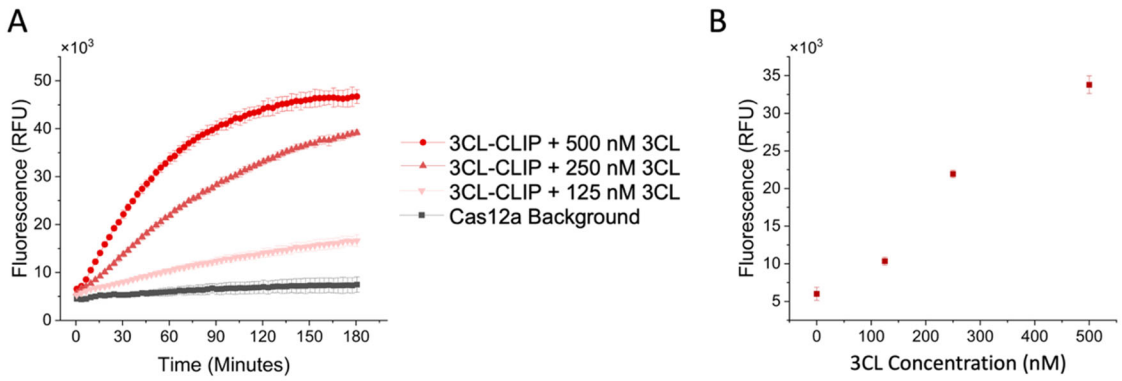

Figure S13. Limit of detection of 3CL via CRISPR-Cas12a assays with 3CL-CLIPs. (A) Time-dependent fluorescence response from 3CL-CLIPs incubated with 500-125 nM of 3CL protease for 30 min. (B) Linear fit of response at 30 min.

6.6 Comparison of CLIP Hairpins with DNA-only Hairpins

CLIPs were designed with 8 base pairs in the stem. As mentioned previously, this length was chosen based on T_m considerations. To compare the function of CLIPs with DNA-only hairpins of similar lengths, we performed CRISPR assays using hairpins made entirely of DNA. We also included controls with the Initiator DNA hybridized to Blocking DNA of different lengths. The contour length of amino acids ranges from 0.36 nm to 0.4 nm, the PEG linker's length is approximately 1.4 nm,[75] and the length of ssDNA is reported to be between 0.3 nm to 0.6 nm per base.[76-78] Therefore, the non-DNA portion of the CLIP (which can be between 6.4-6.8 nm in length if the CLIP has 10 aa) can be approximated using ssDNA containing 10-30 bases.

We used two DNA hairpins in our study. These hairpins are of the form $I_{24}T_{10}B_8$ and $I_{24}T_{30}B_8$. I_{24} represents the initiator strand containing 24 bases. B_8 represents the blocking strand containing 8 bases. $I_{24}T_{10}B_8$ is denoted as DNA Hairpin 10-8 and $I_{24}T_{30}B_8$ is denoted as DNA Hairpin 30-8. Both hairpins have a stem length of 8 base pairs. $I_{24}T_{10}B_8$ has a loop size of $24 - 8 + 10 = 26$ bases. $I_{24}T_{30}B_8$ has a loop size of $24 - 8 + 30 = 46$ bases.

We first examined the impact of different lengths of Blocking DNA on CRISPR signaling when the Initiator and Blocking DNA form intermolecular double strands (**Figure S14**). Our results show that a 24-nt Blocking DNA, fully complementary to the Initiator DNA, completely inhibits CRISPR activation, whereas a 16-nt Blocking DNA, with substantial but incomplete complementarity, does not. This suggests that RNP complexes can bind to partially blocked Initiator DNA through strand displacement when intermolecular double strands are present.

When DNA Hairpin 10-8 and DNA Hairpin 30-8 were used – both containing 8-bp intramolecular double strands – CRISPR activation was observed (**Figure S15**). This indicates that RNP complexes can still engage with partially blocked Initiator DNA via strand displacement, even with intramolecular double strands.

However, when using CLIPs with intramolecular double strands, no CRISPR activation occurred, despite the Blocking DNA being only 8 bases long. This underscores the unique structural properties of CLIPs that prevent strand displacement by the RNP complex, highlighting their distinctive interaction dynamics compared to DNA-only structures.

6.6.1 CRISPR Activation with Initiator DNA Hybridized to 24-nt and 16-nt Blocking DNA

To investigate how blocking the Initiator DNA impacts CRISPR signal, 1 nM of the single-stranded Initiator DNA strand was treated with 10 nM of the 16-nt Blocking DNA or 24-nt Blocking DNA. The 24-nt Blocking DNA fully inhibited CRISPR signal whereas the 16-nt Blocking DNA did not. These results suggest that RNP cannot access fully double-stranded sequences, while, with partial complements, CRISPR-Cas12a can still access the Initiator DNA through toehold-mediated strand displacement.

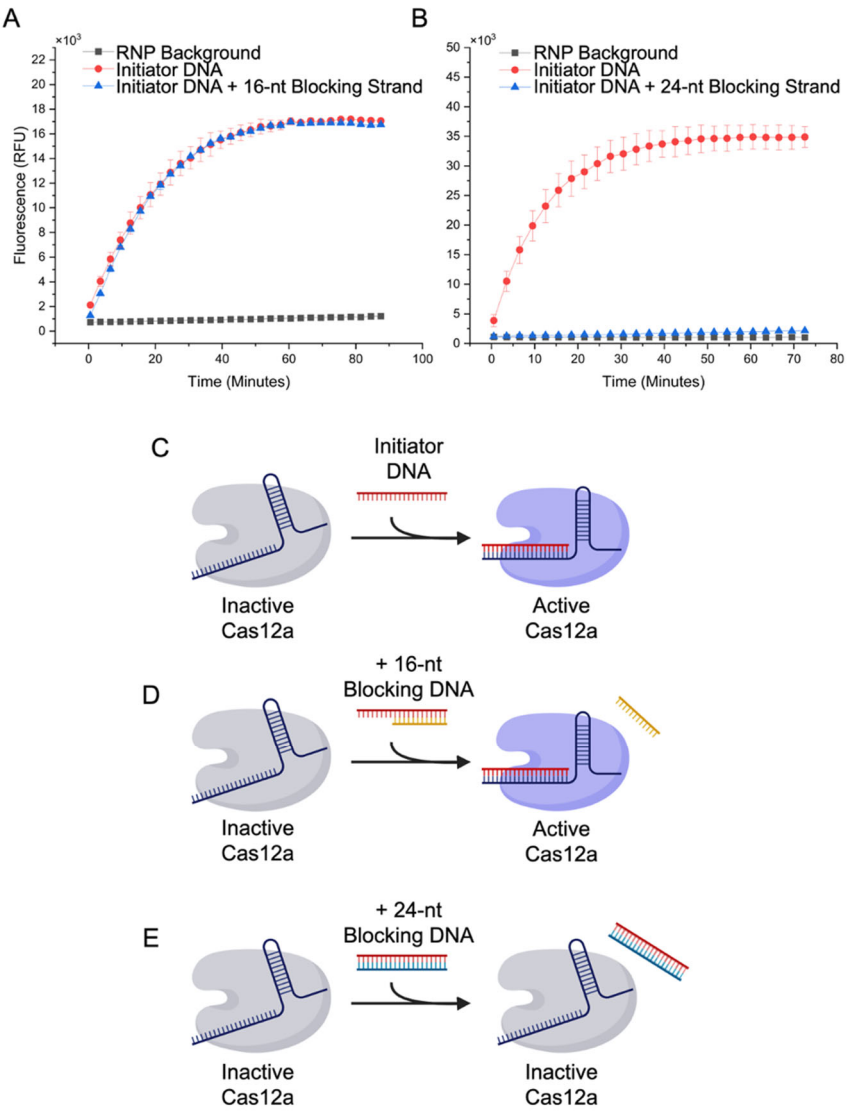

Figure S14. (A) Time-dependent CRISPR assay of Initiator DNA with and without the addition of a partial (16-nt) and (B) a full (24-nt) DNA complement. Scheme showing activation of CRISPR-Cas12a with (C) single stranded Initiator DNA, (D) Initiator DNA treated with the 16-nt Blocking DNA, and (E) Initiator DNA treated with the 24-nt Blocking DNA. Initiator DNA with and without treatment of the 16-nt Blocking DNA can activate CRISPR-Cas12a with no impediment. However, when Initiator DNA is treated with the 24-nt Blocking DNA, CRISPR-Cas12a activation is not observed.

6.6.2 CRISPR Activation with DNA-only Hairpins

CRISPR assays were conducted using 1 nM concentration of DNA Hairpin 10-8 and DNA Hairpin 30-8, both featuring 8-base pair intramolecular hairpins. These hairpins were capable of activating CRISPR, producing fluorescence levels comparable to those from Initiator DNA alone. This demonstrates that the presence of an intramolecular double strand in these hairpins does not hinder CRISPR signaling. In contrast, CLIPs, which also possess an 8-base pair DNA stem, do not activate CRISPR. This difference suggests that the peptide and linker elements incorporated into the CLIPs' loops render them inaccessible to the RNP complex, highlighting a significant structural impact on their functionality.

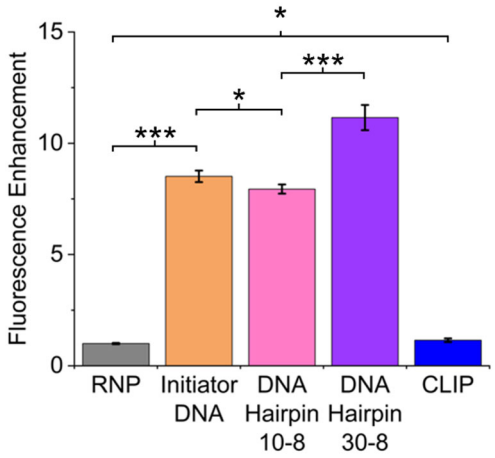

Figure S15. Fluorescence enhancement observed after 5 min when CRISPR RNP and DNase Alert reporters are treated with Initiator DNA, DNA Hairpin 10-8, DNA Hairpin 30-8, and CLIP, respectively. Fluorescence enhancement is calculated as the fluorescence observed relative to the fluorescence of the RNP alone, which is set to a value of 1. *, and *** denote statistical significance at the 95%, and 99.9% confidence levels, respectively, assessed using a one-tailed Student's t-test.

CRISPR assays using DNA Hairpin 30-8 revealed significant insights when Blocking DNA of various lengths were added to the hairpin. Introducing 24-nt Blocking DNA, which is fully complementary to the hairpin's Initiator DNA sequence, effectively inactivates CRISPR (**Figure S16**). This inactivation occurs because the 24-nt Blocking DNA opens the hairpin through toehold-mediated strand displacement (**Figure S18**).

Conversely, adding 16-nt Blocking DNA, which covers only part of the Initiator DNA sequence and not the hairpin stem, initially diminishes the CRISPR signal. Over time, however, the signal increases, resembling a positive cooperativity curve (**Figure S16**). This observation could be attributed to factors such as DNA that is misfolded and not in hairpin form or slow disruption of the hairpin stem by CRISPR-Cas12a due to strand displacement. Once initial activation occurs, the CRISPR-Cas12a enzymes, capable of cleaving ssDNA, begin to degrade the hairpin's loop region. This degradation releases new Initiator DNA, leading to an amplification cycle (**Figure S18**).

In contrast, the loop structure of CLIPs comprises both peptide and DNA, with the DNA portion being part of the Initiator DNA sequence. If CRISPR-Cas12a cleaves this DNA within the loop, the full Initiator DNA sequence is not intact, preventing further activation of CRISPR-Cas12a (**Figure S19**). This structural feature makes CLIPs less susceptible to the amplification cycle typical in DNA-only hairpins, underscoring a significant difference in how CLIPs interact with CRISPR-Cas12a compared to standard DNA hairpins.

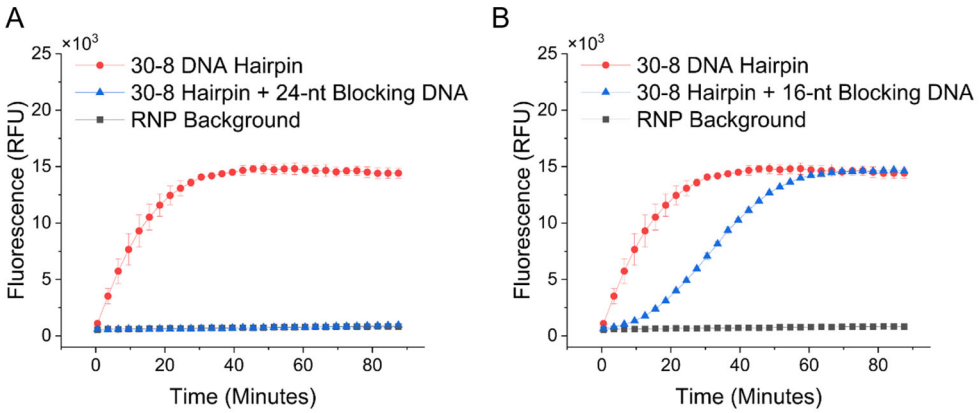

Figure S16. Enhancement of the 30-8 Hairpin with and without the addition of (A) 24-nt blocking DNA and (B) 16-nt blocking DNA. The data displayed represents the average of two measurements, with error bars indicating the deviation between them.

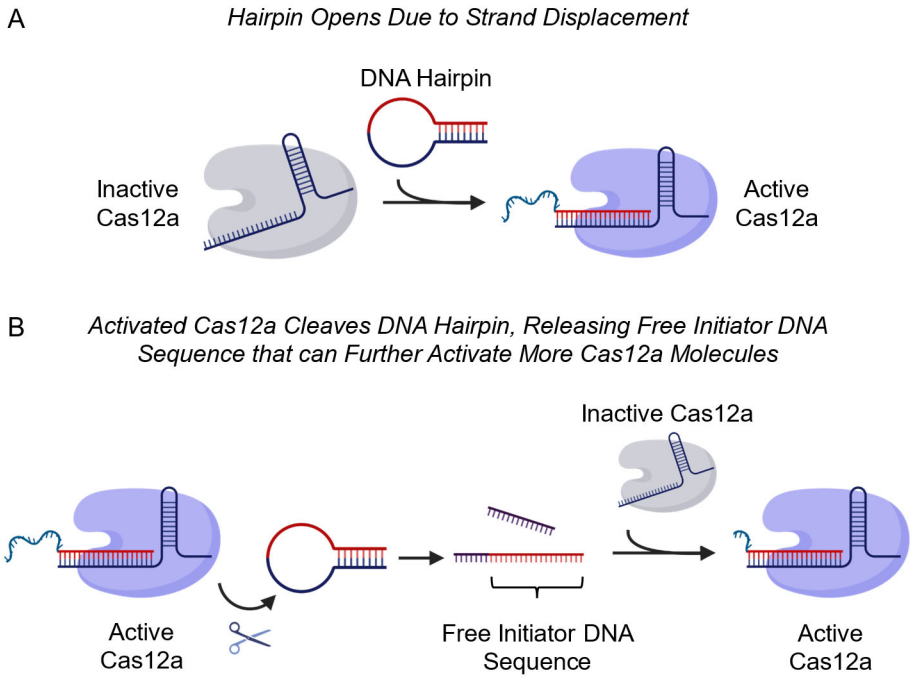

Figure S17. Hypothesized mechanism of activation of CRISPR-Cas12a RNP via DNA hairpins. (A) DNA hairpins may slowly activate Cas12a enzymes due to strand displacement. (B) Active Cas12a enzymes cleave the loop region of DNA hairpins causing them to degrade into new Initiator DNA causing an amplification cycle.

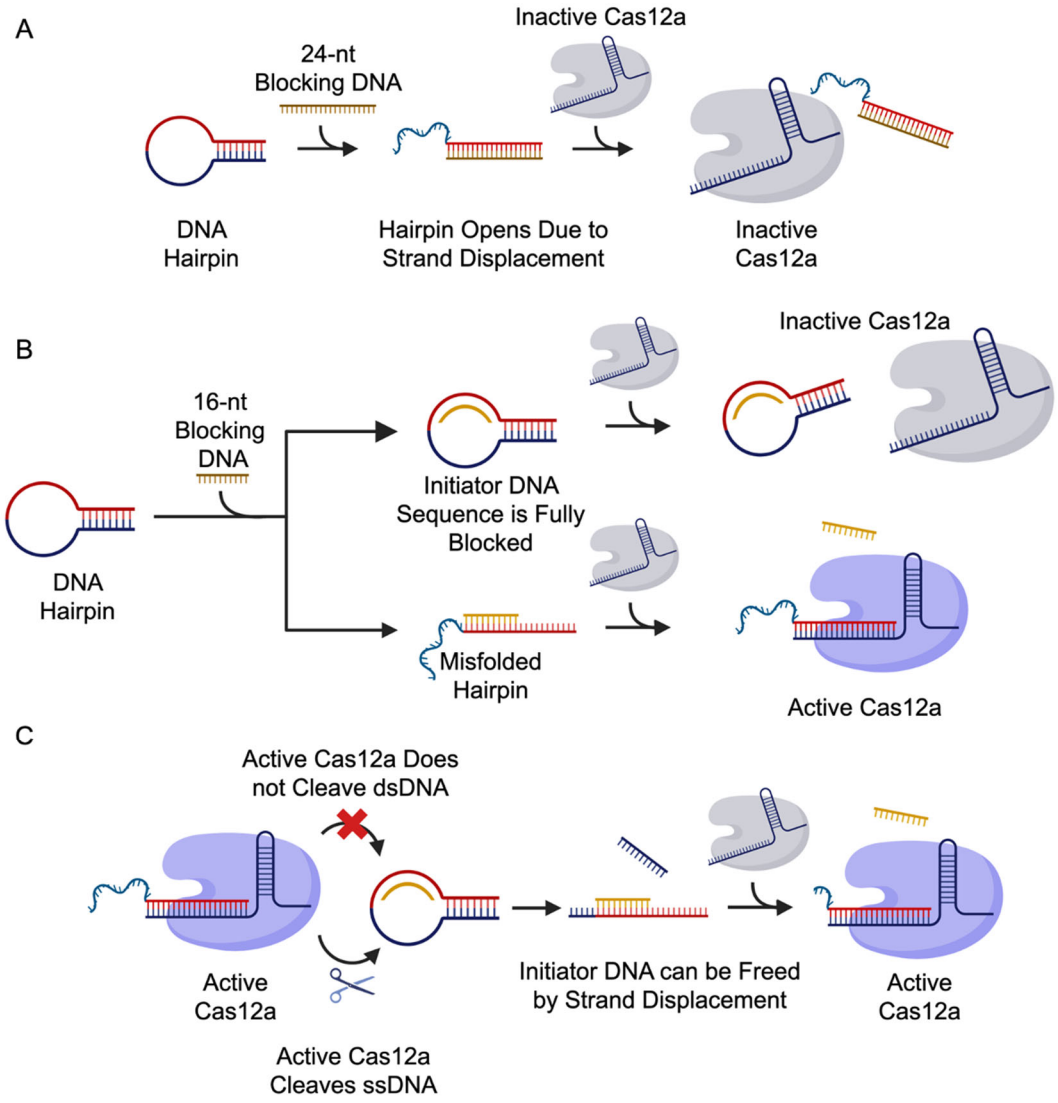

Figure S18. Hypothesized mechanism of activation of CRISPR-Cas12a RNP via DNA hairpins treated with Blocking DNA. (A) Introducing 24-nt Blocking DNA, which is fully complementary to the hairpin's Initiator DNA sequence, effectively inactivates CRISPR. This inactivation occurs because the 24-nt Blocking DNA opens the hairpin through toehold-mediated strand displacement. (B) Adding 16-nt Blocking DNA, which covers only part of the Initiator DNA sequence and not the hairpin stem, initially diminishes the CRISPR signal. Over time, however, the signal increases, resembling a positive cooperativity curve. This observation could be attributed to factors such as DNA that is misfolded and not in hairpin form or slow disruption of the hairpin stem by CRISPR-Cas12a due to strand displacement. (C) With 16-nt Blocking DNA, once initial activation occurs, the CRISPR-Cas12a enzymes, capable of cleaving ssDNA, begin to degrade the hairpin's loop region. This degradation releases new Initiator DNA, leading to an amplification cycle.

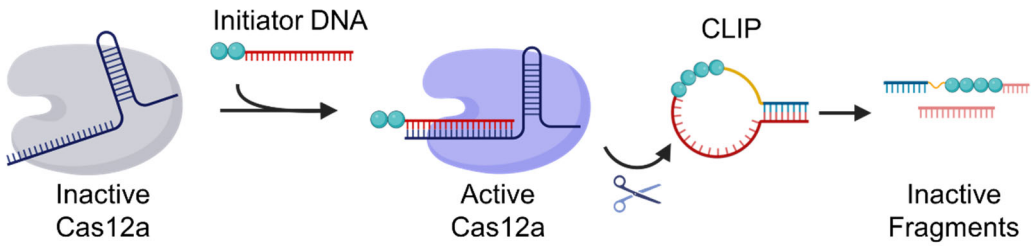

Figure S19. Hypothesized interaction between CRISPR-Cas12a RNP and intact CLIPs. Intact CLIPs in hairpin form do not activate CRISPR. However, upon proteolytic cleavage, CLIPs generate Initiator DNA that can activate CRISPR RNP. Activated CRISPR RNP can potentially cleave intact CLIPs in the ssDNA portion of the hairpin loop. However, in doing so, the Initiator DNA sequence is digested and therefore, it cannot activate additional RNPs. Taken together, non-specific DNA cleavage is not expected to result in background signal from CLIPs.

6.7 Comparison of 3CL-CLIP with Fluorogenic Substrates

To benchmark the ability of CLIPs to detect active proteases, a commercial 3CL protease reporter (3CL-CFP) was employed in this study. 3CL-CFPs were also used to confirm that our purchased proteases are active. Data from these experiments are shown in the main text.

To assess the impact of DNA on enhancing the fluorescence signal, we synthesized a CLIP equipped with a fluorophore (Cy5) and a quencher (BHQ) at opposite ends, designated as FQ-3CL-CLIP. This construct was purified via gel electrophoresis (**Figure S20**) and characterized using UV-Vis spectroscopy (**Figure S21**). The FQ-3CL-CLIP serves as a fluorogenic reporter for the presence of active proteases, as proteolytic cleavage between the fluorophore and the quencher will lead to an increase in fluorescence (**Figure S22**, **Figure S23**).

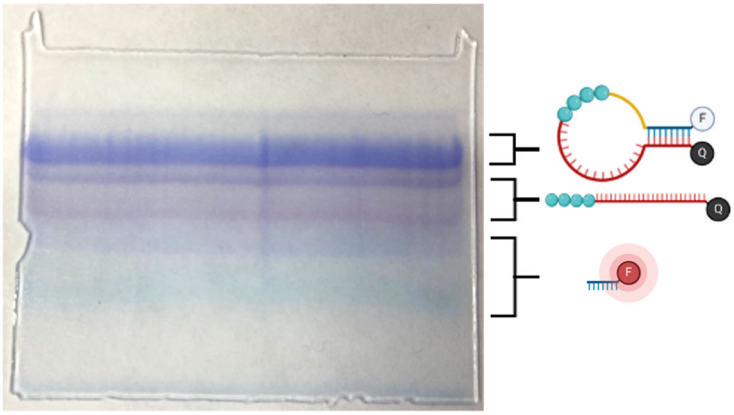

Figure S20. PAGE gel purification of a mixture containing FQ-3CL-CLIPs, unreacted Quencher-labeled Initiator DNA, and Fluorophore-labeled Blocking DNA. Loading was approximately 10 nmol of the desired CLIP. The gel was observed by eye and underwent purification as discussed in **Section 4.5**, to isolate the target CLIP band. The color of each band helps identify its contents: light blue bands suggest Cy5 dye, dark purple bands indicate BHQ, and the top royal blue bands are a mix, showing both Cy5 and BHQ.

UV-Vis spectroscopy was used to support successful synthesis of FQ-3CL-CLIP Probes. A UV-Vis spectrum confirms the presence of DNA, BHQ, and Cy5 due to their characteristic absorbances at 260 nm, ~580 nm, ~650 nm respectively. The absence of DBCO's characteristic 310 nm peak indicates successful conjugation of quencher-DNA linker species and dye labeled blocking strands.

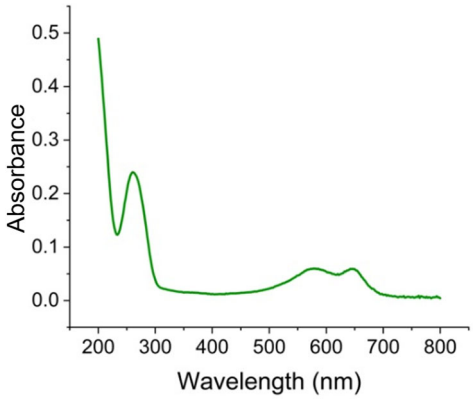

Figure S21. UV-Vis spectra of FQ-3CL-CLIP after gel purification. Characteristic absorbances of DNA, BHQ, and Cy5 at 260 nm, ~580 nm, ~650 nm respectively, are observed while the absence of DBCO's characteristic 310 nm peak indicates successful conjugation of quencher-DNA linker species and dye labeled blocking strands.

Protease-mediated degradation of FQ-3CL-CLIP results in the separation of the fluorophore and the quencher and generates a fluorescence signal. This probe serves as an additional control to support the intended DNA disassociation of CLIPs following proteolytic digestion.

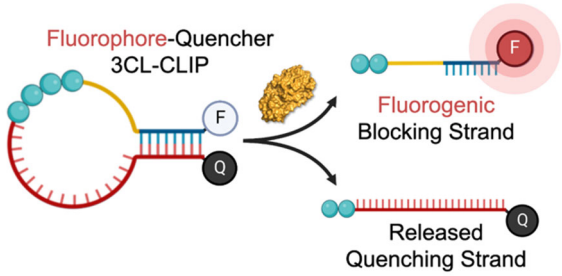

Figure S22. Scheme of Activation of FQ-3CL-CLIPs due to proteolytic cleavage.

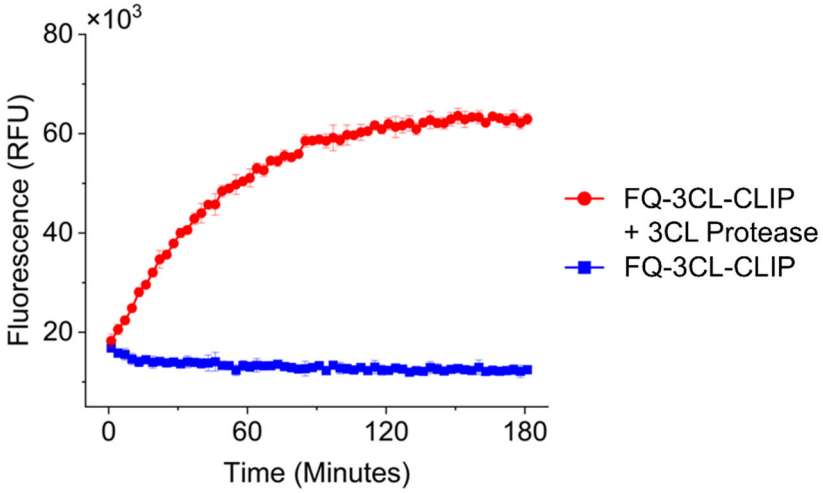

Figure S23. Time-dependent fluorescence assay upon incubation of 100 nM of the FQ-3CL-CLIP with 1 μM 3CL protease in 3CL buffer.

When comparing the fluorescence from the FQ-3CL-CLIP assay with that from a CRISPR assay using 3CL-CLIP, the CRISPR-enhanced 3CL-CLIP exhibited a stronger signal than the FQ-3CL-CLIP, even at concentrations 100 times lower (**Figure S24**). This indicates that DNA effectively amplifies the signal in these assays.

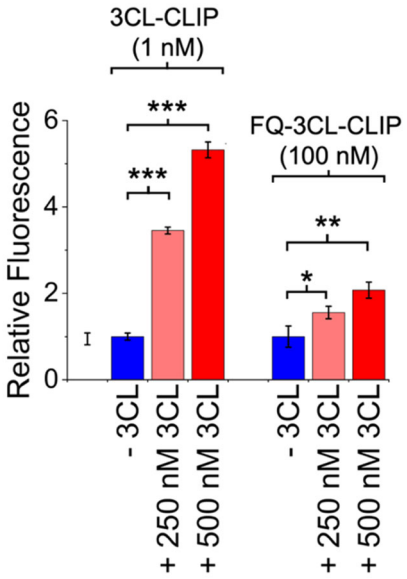

Figure S24. Comparison of fluorescence signal obtained from 3CL-CLIP assays and FQ-3CL-CLIP. Relative fluorescence refers to the ratio of the fluorescence of a sample to the fluorescence of the probe without the 3CL protease. The fluorescence of the probe without 3CL protease set to a value of 1. The final probe concentration in the assay is indicated in the figure. *, **, and *** denote statistical significance at the 95%, 99%, and 99.9% confidence levels, respectively, assessed using a one-tailed Student's t-test.

6.8 Comparison of CTSB-CLIP with Commercial CTSB Probes

Our results show that CTSB-CLIP, at a final concentration of 1 nM, can detect sub-nanomolar concentrations of the protease CTSB. In contrast, a commercial fluorogenic probe for CTSB (CTSB-CFP) failed to detect similar levels of proteases under comparable conditions.

CTSB-CFP and CTSB-CLIP (10 nM) were incubated with 10 nM CTSB protease for 30 min in CTSB buffer. Following this, the samples were diluted 10-fold using CRISPR buffer to a final concentration of 1 nM by probe. In case of CTSB-CLIP, the CRISPR buffer was supplemented with CRISPR-Cas12a RNP and DNase Alert reporters. Fluorescence readings were taken after an additional 120 min.

To determine the limit of detection (LOD) for CTSB-CFP, 1 μM CTSB-CFP was incubated with varying concentrations of CTSB protease (25 nM, 10 nM, 5 nM, 0.1 nM, and 0 nM) in CTSB Buffer for 30 min at 25 °C. After incubation, the samples were diluted 10-fold with CRISPR Buffer, resulting in a final CTSB-CFP concentration of 100 nM during fluorescence measurement in the CRISPR assay. Fluorescence values were plotted as a function of CTSB concentration to generate a calibration curve. The LOD was calculated from the initial slope of this curve using the 3σ/m method and determined to be 3.4 nM.

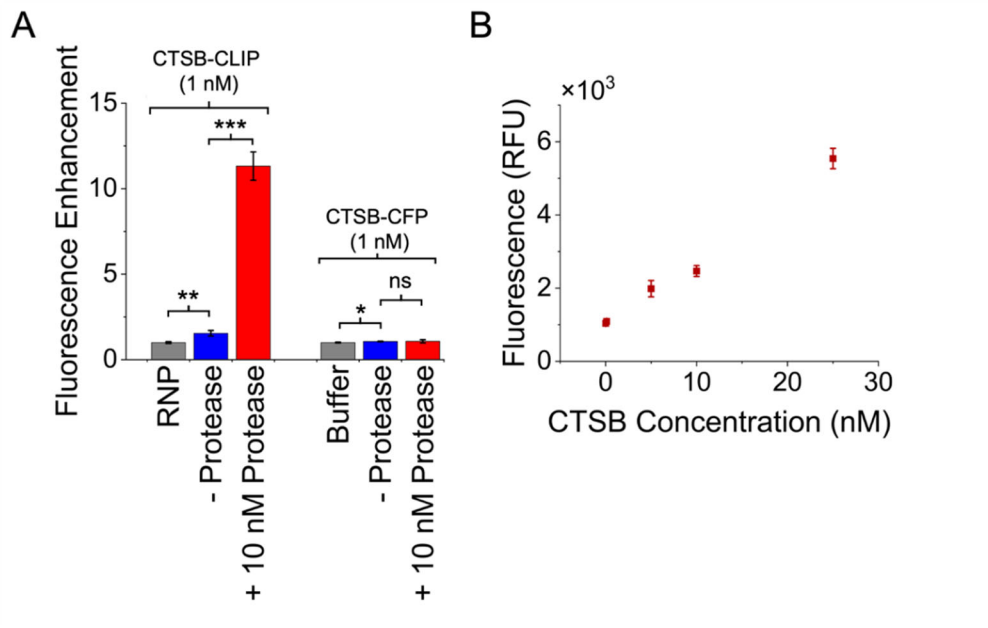

Figure S25. (A) Comparison of fluorescence enhancement when CTSB-CLIP and CTSB-CFP are treated with 10 nM CTSB. Fluorescence enhancement refers to the ratio of the fluorescence of a sample to the fluorescence of the RNP alone, which is set to a value of 1. The final probe concentration in the assay is indicated in the figure. (B) Fluorescence response of 1 μM CTSB-CFP upon incubation with CTSB protease for 30 min. *, **, and *** denote statistical significance at the 95%, 99%, and 99.9% confidence levels, respectively, while "ns" indicates no statistical significance (at the 95% confidence level), assessed using a one-tailed Student's t-test.

6.9 Performance of CLIPs in Complex Media

6.9.1 Stability of CLIPs in the Presence of Nucleases

DNase I was used to assess the stability of CLIP structures against nuclease degradation. DNase I, which digests both single- and double-stranded DNA, was applied to FQ-3CL-CLIP at varying concentrations. Upon digestion, the fluorophore and quencher separate, generating a fluorescence signal indicative of probe degradation. Our results show that after 30 min of treatment, while the CLIP structure is degraded at high DNase I concentrations, it remains stable at DNase activity of 25 U/L or lower, at least up to 30 min. This is more than double the activity of DNAse I in human serum (~10 U/L), demonstrating the robustness of the CLIP structure under relevant scenarios.[66]

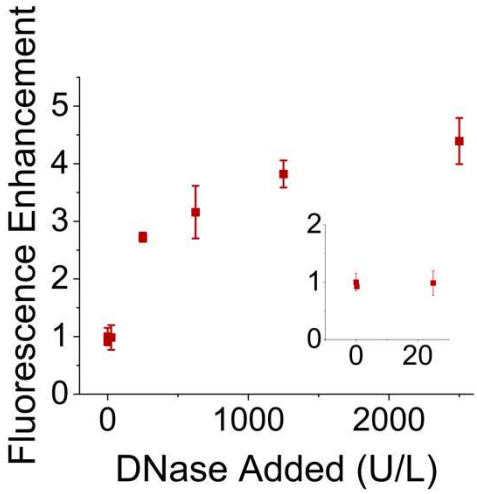

Figure S26. Fluorescence enhancement resulting from FQ-3CL-CLIP being treated with DNase I. Fluorescence enhancement refers to the ratio of the fluorescence of a sample to the fluorescence of the FQ-3CL-CLIP alone, which is set to a value of 1.

6.9.2 Stability of CLIPs in Cell Lysates

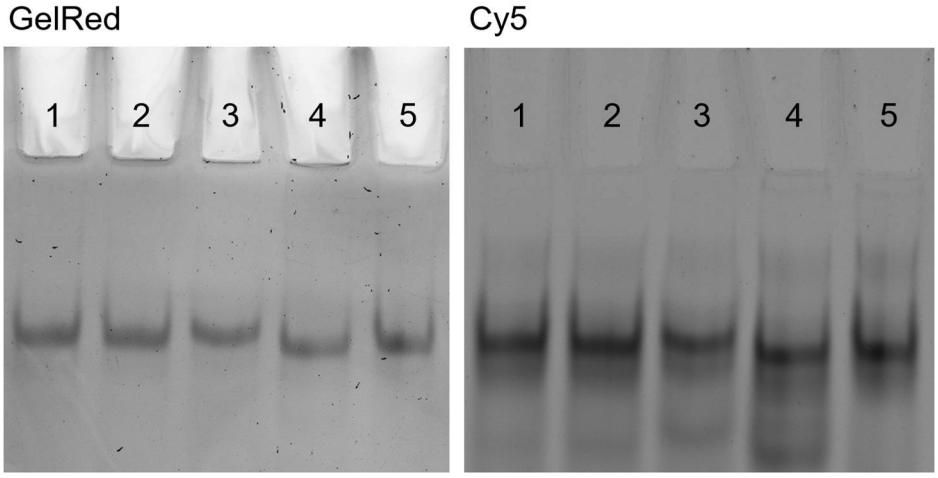

Figure S27. Denaturing PAGE gel of FQ-3CL-CLIPs treated with cell lysates. The gel was imaged in the Cy5 channel, stained with GelRed, and reimaged in the GelRed channel. Bands in the Cy5 channel result from the fluorophore in the FQ-3CL-CLIP whereas bands in the GelRed channel result from the binding of GelRed to the DNA sequences. Panels (1-4) show samples treated with cellular lysates for 30 min, 1 h, 3 h, and 6 h, respectively, while panel (5) shows FQ-3CL-CLIP without cellular lysate treatment. Approximately 2 pmol of each sample was loaded.

It is worth noting that GelRed preferentially stains longer DNA sequences, which explains the presence of only one prominent band in the GelRed channel (the intact CLIP). In the Cy5 channel, faint, faster-migrating bands emerge over time, suggesting progressive degradation of FQ-3CL-CLIP in the cellular lysates. The intact CLIP structure contains both Cy5 and its quencher, BHQ. As the CLIP degrades, Cy5 and BHQ separate, causing an increase in Cy5 fluorescence relative to the intact structure. This artificially enhances the intensity of the fragment bands in the Cy5 channel, making the proportion of fragments appear higher than it actually is. Furthermore, the relatively unchanged intensity of the parent CLIP band in both the GelRed and Cy5 channels indicates that only a small fraction of the CLIP is degraded. Therefore, the CLIP structure is largely stable in cell lysates at least up to 6 h.

6.9.3 Performance of CLIPs in Serum

3CL-CLIP and 3CL-CFP were treated with 3CL protease in the 3CL protease buffer with the addition of 10% human serum. Upon incubation of the probes with serum, it was observed that even without the treatment of the protease there is an increase of background signal of ~200% for both the CLIP and CFP. This indicates that there is a significant background due to perhaps non-specific cleavage of the probe's peptide recognition sequence (which is shared with the CLIP and CFP) by a component in the serum. Upon incubating the probes with 3CL protease, we observed fluorescence increases in both indicating they are working as intended to detect the proteases in the serum.

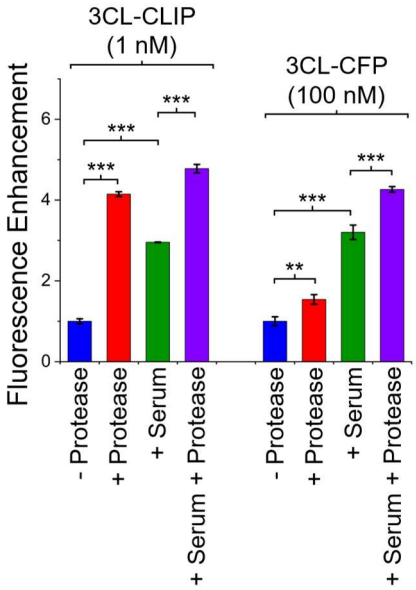

Figure S28. Comparison of fluorescence enhancement from 3CL-CLIP and 3CL-CFP treated with 1 μM 3CL protease, with and without 10% serum. Relative fluorescence is calculated as the ratio of the fluorescence of each sample to that of the probe without protease after 15 min, with the fluorescence of probes without protease set to 1. **, and *** denote statistical significance at the 99%, and 99.9% confidence levels, respectively using a one-tailed Student's t-test.

6.9.4 Performance of CLIPs in Cell Lysates

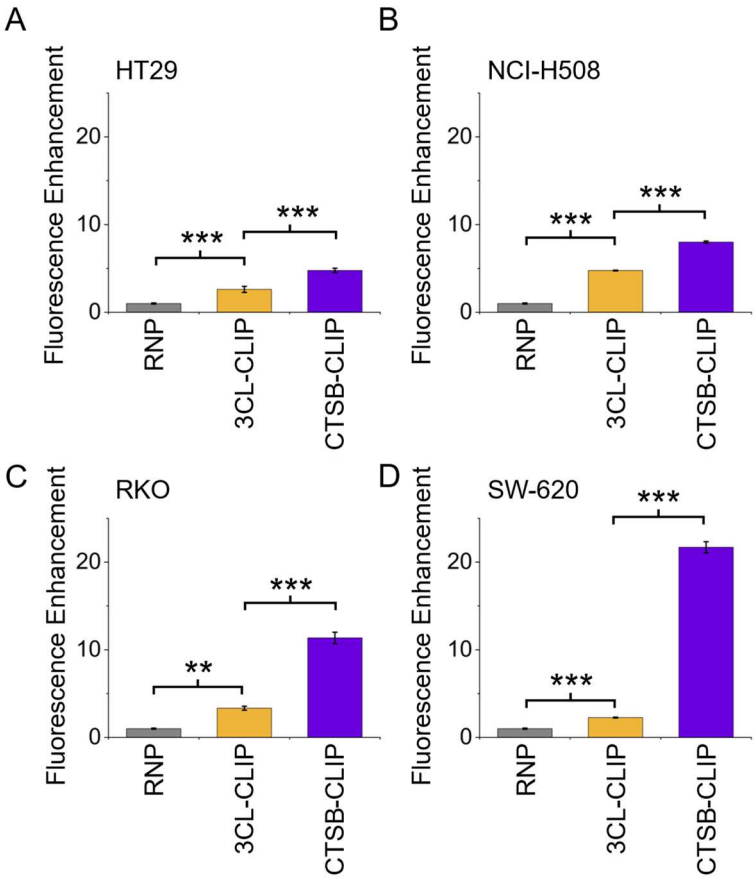

Figure S29. Detection of CTSB using CLIPs in cancer cell lysates. To detect active proteases in complex media, lysates derived from different colon cancer cell lines ((A) HT29,(B) NCI-H508, (C) RKO, and (D) SW-620) were treated with CLIPs. In these cell samples, CTSB is expected to have high activity levels based on previous studies.[60,67,73,74] Therefore, fluorescence from CTSB-CLIP will be correlated to the activity of CTSB protease. On the other hand, the presence of SARS CoV-2 proteases in these samples is not expected. Therefore, the fluorescence from 3CL-CLIP will serve as an estimate of the background in these systems. 10 nM of CLIPs were incubated with 15 µL of the cell lysates (~2 million cells/mL) in a total volume of 45 µL of 1X PBS. The samples were then incubated for 30 min with shaking at RT. Following this, the samples were diluted 10-fold with CRISPR Buffer containing the RNP (final concentration of 10 nM by Cas12a, 10 nM by gRNA, and 2.5 µL/100 µL total solution of DNase Alert). Therefore, the final CTSB-CLIP concentration while reading fluorescence in the CRISPR assay was 1 nM. The fluorescence from the CRISPR assay was read using a plate reader after an additional 30 min (excitation wavelength of 525 nm and an emission at 566 nm). Fluorescence enhancement refers to the ratio of the fluorescence of a sample to the fluorescence of the RNP, which is set to a value of 1. **, and *** denote statistical significance at the 99%, and 99.9% confidence levels, respectively, assessed using a one-tailed Student's t-test.

6.9.5 Limit of Detection of CTSB Protease Using CTSB-CLIP in SW-620 Lysates

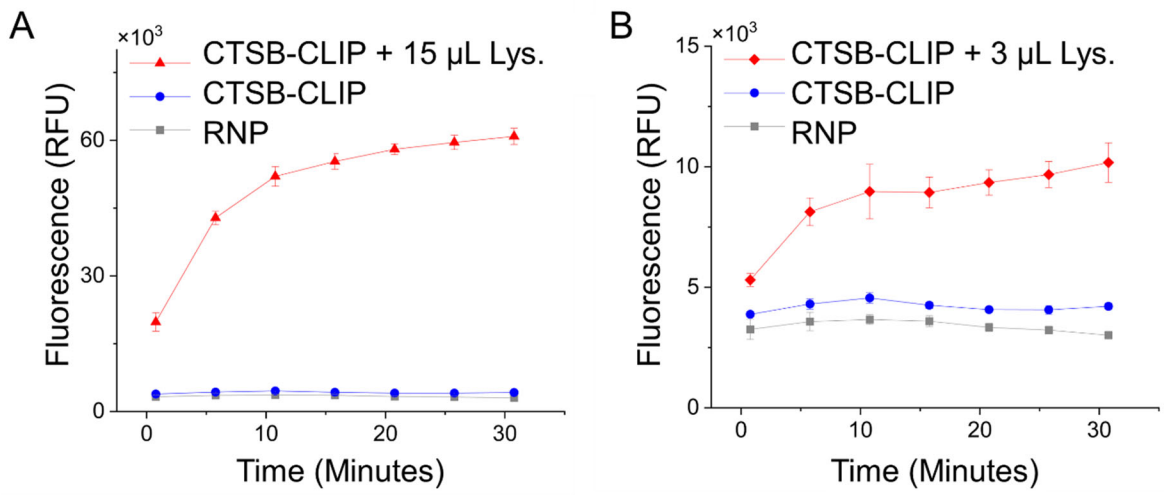

Figure S30. Response of CTSB-CLIP to varying amounts of SW-620 colon cancer cell lysates. 10 nM of CTSB-CLIP was incubated with 0 µL, 15 µL (A), and 3 µL (B) of the cell lysates (~2 million cells/mL) in a total volume of 45 µL of 1X PBS. The samples were then incubated for 30 min with shaking at RT. Following this, the samples were diluted 10-fold with CRISPR Buffer containing the RNP (final concentration of 10 nM by Cas12a, 10 nM by gRNA, and 2.5 µL/100 µL total solution of DNase Alert). Therefore, the final CTSB-CLIP concentration while reading fluorescence in the CRISPR assay was 1 nM. The fluorescence from the CRISPR assay was read over time (excitation wavelength of 525 nm and an emission at 566 nm). It was observed that volumes below 3 µL of cell lysates did not return appreciable responses and therefore the experimental LOD is approximately 6,000 cells.

6.9.6 Detection of CTSB in Cell Lysates Via Commercial CTSB Probe

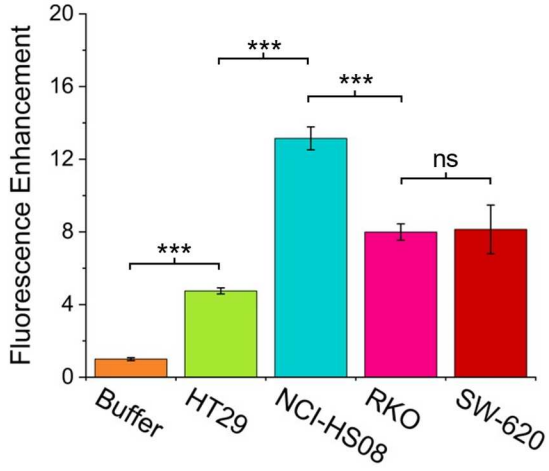

Figure S31. Fluorescence enhancement of CTSB-CFP after incubation with lysates of HT29, NCI-H508, RKO, and SW-620 cell lines. 1 µM of CTSB-CFP was incubated with 15 µL of various cell lysates (~2 million cells/mL) in a total volume of 45 µL of 1X PBS. The samples were then incubated for 30 min with shaking at RT. Following this, the samples were diluted 10-fold with CRISPR Buffer. Therefore, the final CTSB-CFP concentration at fluorescence reading was 100 nM. The fluorescence from CTSB-CFP was read after an additional 30 min (excitation wavelength of 380 nm and an emission at 460 nm). Fluorescence enhancement refers to the ratio of the fluorescence of a sample to the fluorescence of the buffer, which is set at a value of 1. *** denotes statistical significance at the 99.9% confidence level while "ns" indicates no statistical significance (at the 95% confidence level), assessed using a one-tailed Student's t-test.

7 Use of AI language Models in This Paper

The authors note the use of AI language models developed by OpenAI for select parts of this manuscript to check for grammatical mistakes, improve conciseness, or understanding.

8 References

[52] T. MacCulloch, A. Novacek, N. Stephanopoulos, *Chem. Commun.* **2022**, *58*, 4044–4047.

[60] A. Chan, Y. Baba, K. Shima, K. Nosho, D. Chung, K. Hung, U. Mahmood, K. Madden, K. Poss, A. Ranieri, D. S. Shue, R. Kucherlapati, C. Fuchs, S. Ogino, *Cancer Epidemiol. Biomarkers Prev.* **2010**, *19*, 2777–2785.

[66] Y. Kawai, M. Yoshida, K. Arakawa, T. Kumamoto, N. Morikawa, K. Masamura, H. Tada, S. Ito, H. Hoshizaki, S. Oshima, K. Taniguchi, H. Terasawa, I. Miyamori, K. Kishi, T. Yasuda, *Circ.* **2004**, *109*, 2398–2400.

[67] E. Campo, J. Muñoz, R. Miquel, A. Palacín, A. Cardesa, B. F. Sloane, M. Emmert-Buck, *Am. J. Pathol.* **1994**, *145 2*, 301–9.

[73] M. Abdulla, M.-A. Valli-Mohammed, K. Al-Khayal, A. A. Shkieh, A. Zubaidi, R. Ahmad, K. Al-saleh, O. Al-Obeed, J. McKerrow, *Oncol. Rep.* **2017**, *37*, 3175–3180.

[74] L. G. M. Hazen, F. Bleeker, B. Lauritzen, S. Bahns, J. Song, A. Jonker, B. V. Driel, H. Lyon, U. Hansen, A. Köhler, C. Noorden, *J. Histochem. Cytochem.* **2000**, *48*, 1421–1430.

[75] S. R. K. Ainavarapu, J. Brujić, H. H. Huang, A. P. Wiita, H. Lu, L. Li, K. A. Walther, M. Carrion-Vazquez, H. Li, J. M. Fernandez, *Biophys. J.* **2007**, *92*, 225–233.

[76] J. Ambia-Garrido, A. Vainrub, B. M. Pettitt, *Comput. Phys. Commun.* **2010**, *181*, 2001–2007.

[77] A. N. Rao, D. W. Grainger, *Biomater. Sci.* **2014**, *2*, 436–471.

[78] Q. Chi, G. Wang, J. Jiang, *Phys. A: Stat. Mech. Appl.* **2013**, *392*, 1072–1079.